METABOLIC PROFILING OF SUGAR PHOSPHATES USING HPLC-MS WITH MIXED-MODE STATIONARY PHASES

Caroline Emery

Institute of Biological Chemistry and Center for Integrated Biotechnology
Washington State University, Pullman WA, USA

And

Department of Analytical Chemistry
University of Applied Sciences, Sion VS, Switzerland

Under supervision of Mark Lange

Contents

1. Introduction

1.1. Objectives

- Evaluate the utility of SIELC Primesep® B2 (4.6 x 150 mm and 1.0 x 50 mm) columns for the separation of sugar phosphates.
- Evaluate the utility of SIELC Primesep® SB (4.6 x 150 mm and 1.0 x 50 mm) columns for the separation of sugar phosphates.
- Optimize detection of sugar phosphates using an ion-trap MS detector.
- Calibrate detector for different sugar phosphates.
- Test various sugar phosphate analogues with regard to their utility as an internal standard.
- Quantify sugar phosphates in an extract from tobacco leaf.

1.2. HPLC-MS

1.2.1. High-performance liquid chromatography (HPLC):

High-performance liquid chromatography is a separation technique based on the interactions of the analytes with the stationary phase (solid column material). The intrinsic properties of the compounds (size, structure…) and the affinity with the stationary phase (polarity…) influence the time the compounds need to migrate through the column.
Four different separation mechanisms are known: surface adsorption, partition, ion-exchange and exclusion. In each chromatographic technique, one of the four mechanisms predominates, but it should be emphasized that two or more may be involved simultaneously. The choice of the technique to use depends principally on the sample matrix and the compounds that need to be separated.

[1-2]

Figure 2 shows the main components of HPLC instrumentation.

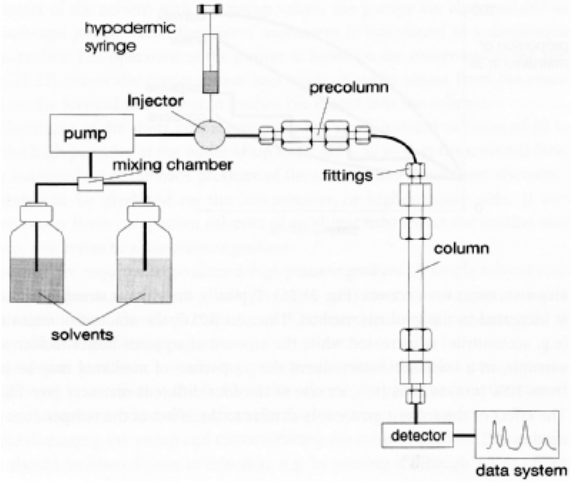

Figure 1: Structure of an HPLC unit with a pre-column. [1]

In reverse-phase mode, the surface chemistry of the stationary phase has nonpolar characteristics. The polarity of the mobile phase can be varied by mixing one or more organic solvents (such as MeOH or ACN) with water or aqueous buffers.
One of the limitations of reversed-phase columns is the lack of retention of highly polar compounds. Novel mixed-mode stationary phases promise to alleviate this limitation. Retention comes from two available interactions: reverse-phase (due to hydrophobic interactions) and ion-exchange (due to electrostatic interactions). [3]

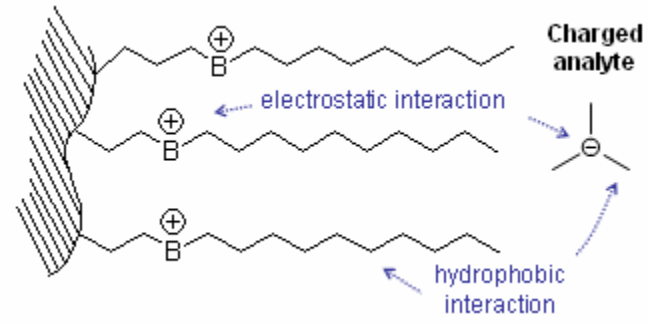

Figure 2: Retention schematic in mixed-mode phase [3]

1.2.2. Mass spectrometry (MS):

Mass spectrometry is an analytical technique based on the generation of ions in gaseous phase. The ions are separated or filtered according to their mass-to-charge ratio (m/z) and detected. This technique is extremely sensitive, thus making it amenable to quantitative trace analysis.
Nowadays, the mass spectrometer is a very sophisticated and computerized instrument. It consists of 5 parts: sample inlet, ionization chamber, mass analyzer, ions detector and a data analysis system.

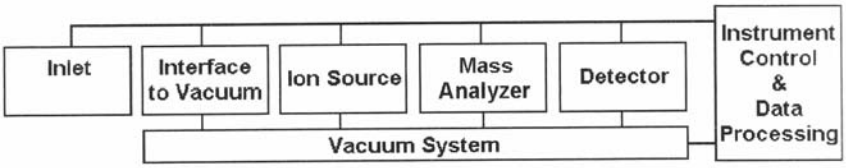

Figure 3: Conventional MS diagram [1]

There are several different ionization techniques (electrospray ionization, atmospheric pressure chemical ionization and desorption ionization) and five different analyzers (magnetic analyzers, quadrupole analyzers, ion trap analyzers, Time-of-flight analyzers and Fourier-transform analyzers). Analyte detection is usually achieved with electron multipliers such as dynode multipliers.
An important factor in mass spectrometry is the quality of the vacuum, to avoid unwanted collisions.

The quadrupole ion trap consists of a cylindrical ring electrode to which the quadrupole field is applied, and two endcap electrodes. Make-up helium gas is generally added from the collision gas lines and serves an important role in stabilizing the ions in their orbits. Ion orbital stability is also improved by applying axial modulation (voltage applied between the ionization electrode and the exit electrode at a frequency about one-half that of the center of the ring electrode voltage). This has the effect of moving the ions away from the center of the trap, where the voltage is zero. The analysis is performed by gradually increasing the ring electrode's scanning voltage.

[1-4-5-6-7]

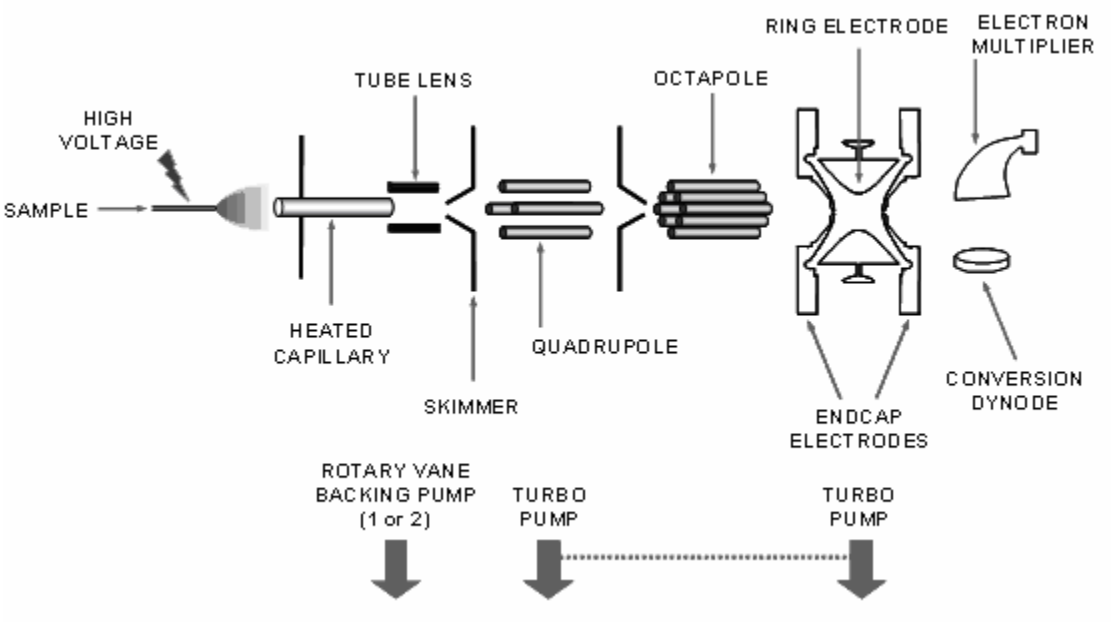

Figure 4: Ion trap MS schematics
[http://pcf.epfl.ch/page58372.html]

1.2.3. Coupling HPLC and MS:

Combining LC and MS offers the possibility of taking advantage of both LC as a powerful separation technique and MS as a powerful and sensitive detection and identification technique. However, major problems occurred initially when both were coupled.

The first apparent problem was the introduction of the LC flow (usually 1 ml/min) into the MS. The use of nano-HPLC was necessary to obtain really small flow rates but, in the meantime, the development of redesigned LC-MS interfaces has made the use of normal LC flow rates possible.
The mobile phase composition can also be a problem, because it can result to an overloading of the MS with charges salt ions. The MS system usually does not permit the introduction of large amounts of nonvolatile material such as

phosphate buffers or other ion-pairing agents. That problem is principally solved by replacing the nonvolatile buffers with volatile ones.
The non volatility of the analytes could also have been considered as a problem. But nowadays, alternative ionization methods (e.g. APCI and APPI) have been introduced and solved that problem.

The electrospray interface is a powerful soft ionization method resulting in limited fragmentation, which is recommended for use with highly polar and charged materials. Ionization is accomplished by passing the eluent down a heated metal capillary tube along which an electric charge differential is applied. The evaporating liquid is sprayed out as charged droplets which decrease rapidly in size.

[1-4-5-6-7]

1.3. Photosynthesis in C_3-plants

Photosynthesis is an essential biochemical process that allows plants to capture solar energy for conversion of carbon dioxide and water into fixed carbon and oxygen.
The simple general equation for photosynthesis is:

$$6\ CO_2 + 12\ H_2O + \text{photons} \rightarrow C_6H_{12}O_6 + 6\ O_2 + 6\ H_2O$$

carbon dioxide + water + light energy → glucose + oxygen + water .

Photosynthesis occurs in two stages:

1. In the first phase, light-dependant reactions or photosynthetic reactions (also called the *Light reactions*) capture the energy of light and use it to make high-energy molecules.
2. During the second phase, the light-independent reactions (also called the Calvin-Benson cycle, and formerly known as the *Dark reactions*) use the high energy molecules to capture CO_2 and generate the precursors of glucose.

Both sets of reactions are contained within the chloroplast of higher plants.

1.3.1. Light reactions:

The reactions of photosynthesis convert the energy of light into chemical energy. More precisely, light energy powers the oxidation of water by starting a flow of electrons that leads to the reduction of nicotinamide adenine dinucleotide phosphate (NADP) to NADPH (Fig. 5).

In addition, photosynthetic reactions serve to create a proton gradient across the chloroplast membrane. Its dissipation is used for the concomitant synthesis of adenosine triphosphate (ATP), the universal energy currency of the cell.
The two high-energy molecules NADPH and ATP are then used to feed the carbon fixation (Calvin-Benson) cycle.

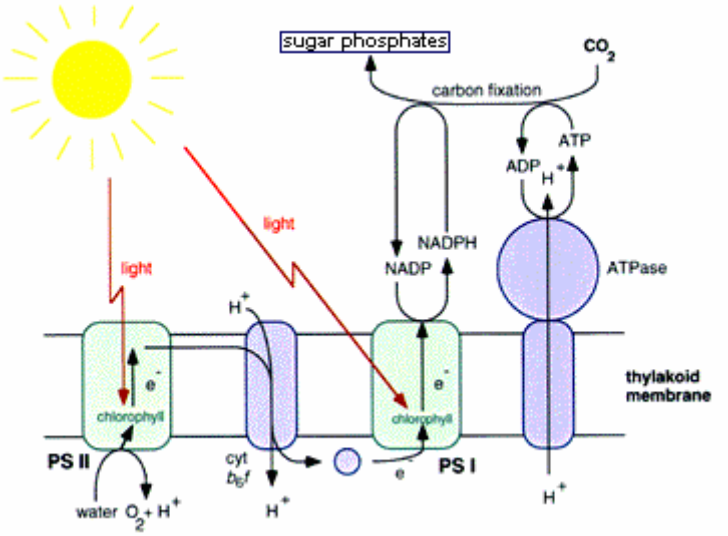

Figure 5: Overview of photosynthetic processes as they occur in plants [http://photoscience.la.asu.edu/photosyn/education/photointro.html]

1.3.2. Dark reactions:

The light-independent stage is a series of 14 enzymatic steps involving 12 enzymes. The first step catalyzed by RuBisCO (ribulose 1,5-bisphosphate carboxylase/oxygenase) uses only RuBP and CO_2. The enzyme RuBisCO captures CO_2 from the atmosphere and releases three-carbon sugars which are later combined to form various sugar phosphates.

Three different pathways of carbon fixation occur in the plant kingdom. C_3 carbon fixation is the most common (C_3 plants represent approximately 95% of Earth's plant biomass). C_4 carbon fixation and CAM (Crassulacean Acid Metabolism) contain supplementary pathways to concentrate or store CO_2 in leaf tissue during the day or at night, respectively.

1.3.3. Carbon reactions in C_3 plants:

As the first stable product in the multistep conversion of CO_2 into sugar phosphates, most plants produce a three-carbon compound, 3-phosphoglycerate (3-PGA). More specifically, the carboxylation of a five carbon sugar, ribulose 1,5-bisphosphate (RuBP), produces a C_6 intermediate that is immediately cleaved into two molecules of 3-PGA.

$$6\ CO_2 + 6\ RuBP \rightarrow 12\ 3\text{-}PGA$$

This reaction occurs in all plants as the first step of the Calvin-Benson cycle (Fig. 6) and is catalyzed by the enzyme RuBisCO (the most abundant enzyme on Earth). This phase of the cycle is called *carboxylation*.

Reduction is the second phase of this process. This two-step reductive phase converts 3-PGA into the triose phosphates, glyceraldehyde-3-phosphate (GAP) and dihydroxyacetone phosphate (DHAP). PGA kinase and then GAP dehydrogenase catalyze the all process and ATP and NADPH are both required in this phase of the cycle. The triose phosphates can either be transported to the cytosol to form sucrose or used for regeneration. (Fig. 6)

The *regeneration* steps involve a number of transketolase reactions, which eventually yield 5 carbon sugar phosphates that interconvert to form RuBP.
In addition, a hexose monophosphate, fructose-6-phosphate (F6P), is also formed by splitting off one P_i from fructose-1,6-bisphosphate (FBP), which itself is formed by addition of GAP and DHAP. In this process, additional ATP is consumed (Fig. 6).

Because five GAP are used in the regeneration phase, the addition of three molecules of CO_2 to the C_5 sugar RuBP is necessary to form one hexose phosphate. Thus, the total energetic requirement for the synthesis of one molecule of hexose phosphate is nine molecules of ATP and six molecules of NADPH.

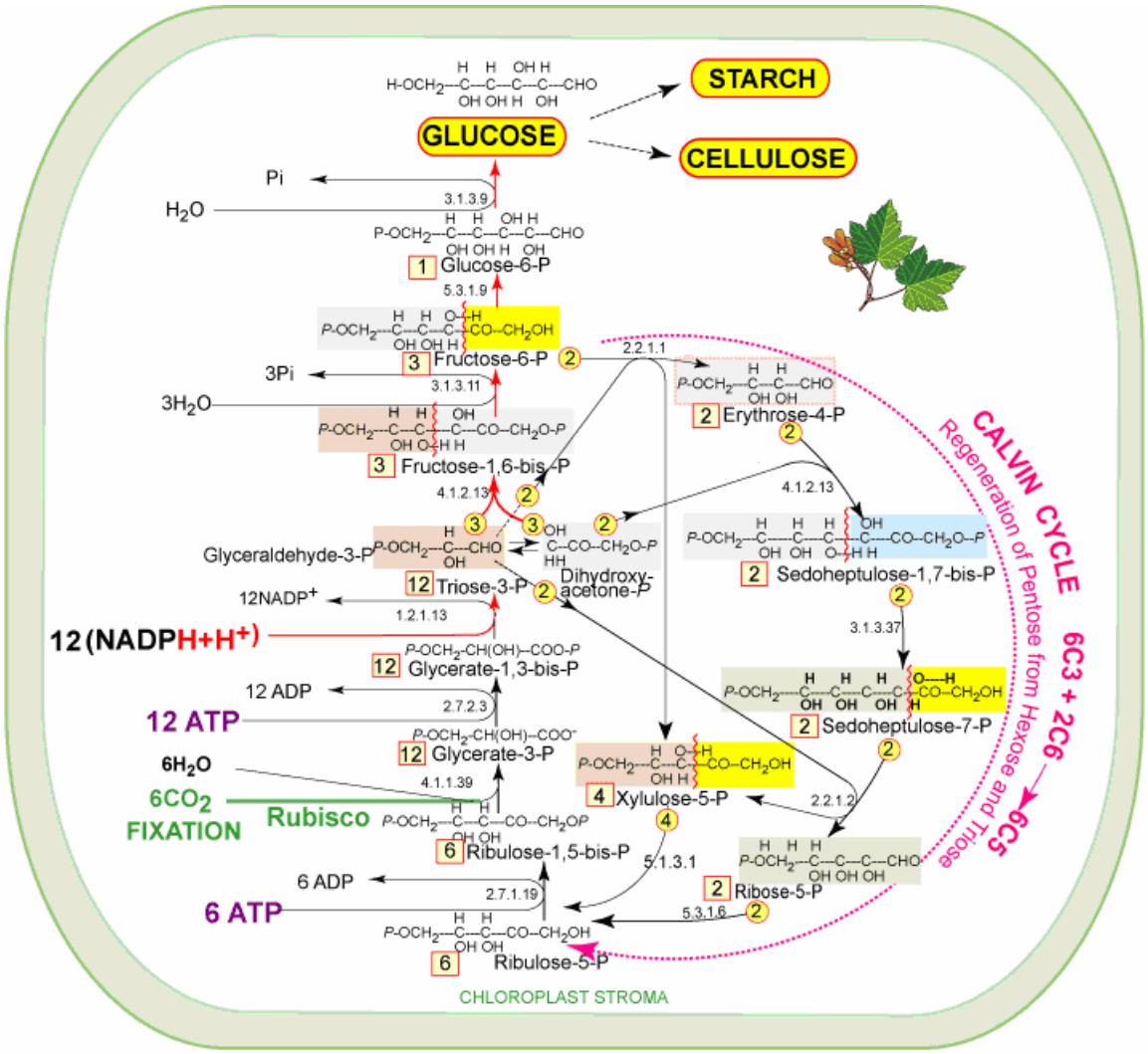

Figure 6: The Calvin-Benson Cycle
[http://www.tcd.ie/Biochemistry/IUBMB-Nicholson/gif/27.gif]

The analysis of sugar phosphates is relatively complicated because of their instability, their chromatographic/mass-spectrometric behavior and their low concentrations in biological samples. Some of the most common sugar phosphates have isomers that are isobars and their MS fragmentation patterns are very similar, thus making chromatographic separations necessary. Conventional reversed phase HPLC has so far been ineffective and ion-pair chromatography provides only a partial separation and requires long equilibration times. [12]

The here presented work uses novel mixed-mode stationary phases for the separation of RuBP, glycerate 3-phosphate or 3-phosphoglyceric acid (PGA), dihydroxyacteone phosphate (DHAP), fructose 1,6-bisphosphate (FBP), fructose 6-phosphate (F6P), glucose 6-phosphate (G6P) and ribose 5-phosphate (R5P).

2. Experimental

2.1. Chemicals and reagents

Table 1: Chemicals and reagents [Merck ChemDat: http://pb.merck.de]

NAME	ACRONYM	PURITY	ORIGIN	WARNINGS
Reference Standards				
Dihydroxyacetone phosphate dilithium salt $C_3H_5Li_2O_6P$	DHAP	≥95%	Sigma D-7137	
D-Fructose 1,6-bisphosphate tetra(cyclohexyl-ammonium) salt $C_6H_{14}O_{12}P_2 \cdot 4C_6H_{13}N$	FBP	≥95%	Sigma F-0752	
D-Fructose 6-phosphate disodium salt hydrate $C_6H_{11}Na_2O_9P \cdot xH_2O$	F6P	~98%	Sigma F-3627	Harmful by inhalation, in contact with skin and if swallowed; possible risk of irreversible effects.
D-Glucose 6-phosphate disodium salt hydrate $C_6H_{11}\ Na_2O_9P$	G6P	98-100%	Sigma G-7250 (before Jan 2007)	
D-Glucose 6-phosphate sodium salt $C_6H_{11}NaO_9P$		98%	Aldrich 285978 (after Dec 2006)	
D-(−)-3-Phosphoglyceric acid disodium salt $C_3H_5Na_2O_7P$	PGA	~95%	Sigma P-8877	Harmful by inhalation, in contact with skin and if swallowed; possible risk of irreversible effects.
D-Ribose 5-phosphate disodium salt hydrate $C_5H_9Na_2O_8P \cdot xH_2O$	R5P	≥98%	Sigma R-7750	
D-Ribulose 1,5-bisphosphate sodium salt hydrate $C_5H_{12}O_{11}P_2 \cdot xNa^+ \cdot yH_2O$	RuBP	~90%	Sigma R-0878 (before Jan 2007)	Toxic by inhalation, in contact with skin and if swallowed; irritating to eyes, respiratory system and skin.
		≥99.0%	Fluka 83895 (after Dec 2006)	

NAME	ACRONYM	PURITY	ORIGIN	WARNINGS
			Solvents	
ACN CH_3CN	ACN	>99.99%	OmniSolv AX0151-1 (before Jan 2007) OmniSolv AX0156-1 (after Dec 2006)	Highly flammable; harmful by inhalation, in contact with skin and if swallowed; irritating to eyes.
Water H_2O	H_2O	High purity for HPLC	Burdick & Jackson Cat. 365-4 (before Jan 2007) OmniSolv WX0004-1 (after Dec 2006)	
Methanol CH_3OH	MeOH	>99.9%	OmniSolv MX0488P-1	Highly flammable; toxic by inhalation, in contact with skin and if swallowed; toxic: danger of very serious irreversible effects through inhalation, in contact with skin and if swallowed.
Tetrahydrofuran C_4H_8O	THF	>99.99%	OmniSolv TX0279P-1	Highly flammable; may form explosive peroxides; irritating to eyes and respiratory system.
			Others	
AmFm CHO_2NH_4	AmFm	99.995+%	Sigma-Aldrich 516961	Irritating to eyes, respiratory system and skin.
Formic acid CH_2O_2		~98% 98%	Fluka 56302 (before Jan 2007) EMD FX0440-7 (after Dec 2006)	Flammable; causes severe burns.

2.2. Instrumentation

- usual laboratory's material
- pH meter 430, Corning (relative accuracy: ± 0.01)
- LC/MSD trap Agilent 1100 Series :
    - Quaternary pump G1311A
    - Micro vacuum degasser G1379A
    - Thermostatted autosampler G1367A

- ESI source G1948A
- Ion trap mass spectrometer Agilent G2445

- HPLC columns:
  - SIELC Primesep® B2 4.6 x 150 mm, 5 µm 100Å
  - SIELC Primesep® B2 1.0 x 50 mm, 5 µm 100 Å
  - SIELC Primesep® SB 4.6 x 150 mm, 5 µm 100 Å
  - SIELC Primesep® SB 1.0 x 50 mm, 5 µm 100 Å

  Primesep® B2 and SB columns are reverse-phase analytical column with strong embedded basic ion-pairing groups.

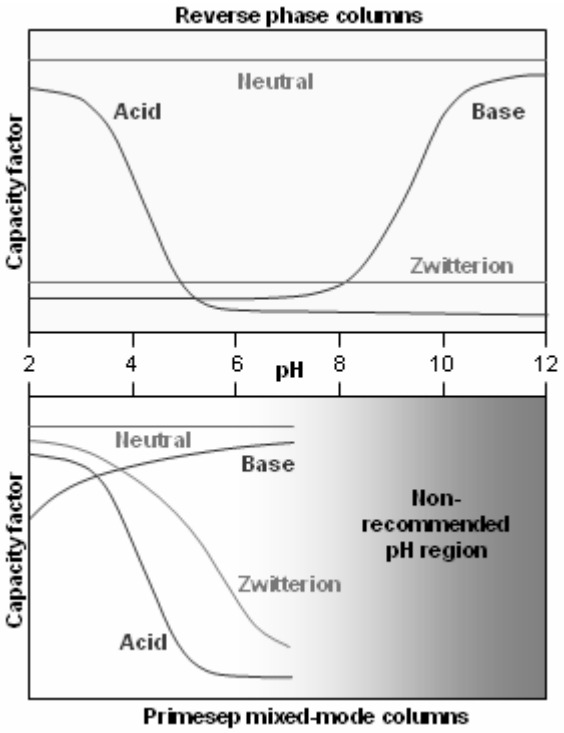

Advantages:

- Improved retention of acidic compounds by anion-exchange mechanism.
- Separation of bases by ion-exclusion mechanism.
- Retention of neutral compounds by reverse-phase mechanism.
- All mobile phases are compatible with LC-MS and preparative chromatography (working pH range from 1.5 to 7 for B2 and 1.5 to 5 for SB).

[3]

2.3. Buffer solutions

The buffer solution is made by diluting 6.32 g of AmFm in water. The target pH values (2, 2.5, 3 and 3.5) are then adjusted with formic acid.
Before being used with the HPLC-MS, the solution is filtered using a nylon filter (0.45 µm).

2.4. Preparation of standards

For the separation optimization, a stock solution containing about 0.1 % (~$4 \cdot 10^{-3}$ M) of each standard in water is prepared.

When not in use, all the solutions were stored at -20°C, and each solution was filtered using a nylon filter (0.45 µm) before being used with the HPLC-MS.

Preparation of the stocks solutions:

Some standards (F6P, R5P and RuBP) contain an undefined amount of water. Thus, all standards were dried by desiccation (silica gel) at -20°C for 2 days. This procedure was performed only once, because most of the sugar phosphates are quite unstable.

Then, the standards were weighed to obtain a concentration of roughly $8 \cdot 10^{-3}$ mol/l, and dissolved in 10 ml high purity water. For FBP and RuBP, the concentration is about $4 \cdot 10^{-3}$ mol/l, because the quantity available was smaller. The masses (m) and molarities (M) of each stock solution are reported in Table 2.

Table 2: Standards preparation (stock solutions)

SUGAR PHOSPHATES	Ref.# [Sigma]	PURITY %	$m_{lost\ during\ dessication}$ [%]	$m_{stock\ solution}$ [mg]	$M_{stock\ solution}$ [mol/l]
G6P	285978	98	7	23.2	$8.22 \cdot 10^{-3}$
F6P	F3627	~98	0	26.0	$8.55 \cdot 10^{-3}$
R5P	R7750	≥98	4	23.4	$8.54 \cdot 10^{-3}$
DHAP	D7137	≥95	6	15.1	$8.30 \cdot 10^{-3}$
PGA	P8877	~95	1	19.2	$8.35 \cdot 10^{-3}$
FBP	F0752	≥95	11	29.0	$3.94 \cdot 10^{-3}$
RuBP	83895	≥99.0	3	18.8	$4.68 \cdot 10^{-3}$

Because the standards have an approximate purity and because we could not get any further information concerning the exact purity, the calculation of the molarities is made considering a purity at 100%.

MS optimization:

For the MS optimization, the standards had to be dissolved in a specific eluent composition. This composition had to be the same as the eluent composition when analytes reach the detector during the separation. Thus, the solutions were diluted with a certain volume (V) of ACN and AmFm 100 mM pH 2. Then, those solutions were diluted with the same eluent composition to obtain lower concentrations.

All the operations made for each standard are reported in Table 3.

Table 3: Solutions preparation for the MS optimization

SUGAR PHOSPHATES	ELUENT COMPOSITION	$V_{stock\ solution}$ [µl]	V_{ACN} [µl]	V_{AmFm} [µl]	DILUTION	M [mol/l]
G6P	15% AmFm 21% ACN 64% H_2O	1920	630	450	5X	$1.05 \cdot 10^{-3}$
F6P						$1.09 \cdot 10^{-3}$
R5P						$1.09 \cdot 10^{-3}$
DHAP						$1.06 \cdot 10^{-3}$
PGA	30% AmFm 21%ACN 49% H_2O	2450	1050	1500	5X	$0.82 \cdot 10^{-3}$
FBP	50% AmFm 10% ACN 40% H_2O	2000	500	2500	2X	$0.79 \cdot 10^{-3}$
RuBP						$0.94 \cdot 10^{-3}$

External calibration:

For the external calibration, the stock solution was diluted 50 times with the initial eluent of the separation (15% AmFm 100 mM pH 2 and 21% ACN). Then the solution was diluted further so that the following concentrations were obtained.

Table 4: Concentrations for the calibration

c [mol/l]		COMMENTS
~$160 \cdot 10^{-6}$	1	dilution 50x (or 25x) from stock solution
~$80 \cdot 10^{-6}$	2	dilution 2x from 1
~$40 \cdot 10^{-6}$	3	dilution 2x from 2
~$20 \cdot 10^{-6}$	4	dilution 2x from 3
~$10 \cdot 10^{-6}$	5	dilution 2x from 4

2.5. HPLC-MS methods

During the separation optimization, some parameters of the analysis stayed constant. In Table 5, these parameters are listed.

Table 5: Constant HPLC-MS parameters

PARAMETERS	PRIMESEP® B2 COLUMN	PRIMESEP® SB COLUMNS
Sampler temperature	4°C	
Column temperature	4°C	
Injection Volume	10 µl	
Injection Mode	Needle wash, 3 s.	Needle wash, 1 s.
Column Flow	1.0 ml/min	0.6 ml/min
Solvent A	water	
Solvent B	MeOH	MeOH or THF
Solvent C	AmFm 100 mM pH 3	AmFm 100 mM pH 2
Solvent D	ACN	
Ion Polarity	Negative	
Drying gas temperature	325°C	

Nebulizer	15.00 psi		50.00 psi
Drying Gas	5.00 l/min		8 l/min
High voltage capillary		3500 V	
Scan		50-400 m/z	
Averages		7 spectra	
ICC Target	20000		10000
MS Mode		AutoMS(2)	
Ions searched	259, 229, 169 (339), 185 (371), 339 and 309 m/z		

The dead time (t_0) was determined by the injection of MeOH and detection with a DAD detector at 254.5 nm.

2.6. Analyses overview

Among the Primesep® B2 columns only the 4.6 x 150 mm was used, because the separation with this column was not satisfactory and the smaller sized column (1.0 x 50 mm) was not evaluated at all. The different analyses made using Primesep® B2 4.6 x 150 mm column are listed in Table 6.

Table 6: Optimization of the sugar phosphates separation with SIELC Primesep® B2 4.6 x 150 mm column

	ELUTION CONDITION	ANALYSIS NAMES
TESTS pH(AmFm) 3 and 2.5	Isocratic; AmFm 15%, ACN 10% and MeOH 10%	1002_02 & 1002_04
TESTS GRADIENT (see Appendix A)	Gradient	1010_02-06-08-09 1011_02 to 06 1012_02-03
WINDOW DIAGRAMS AmFm 5 to 50%	Isocratic; MeOH 10% and ACN 10%	- 1004_11 to _18 (_14 is a blank) - 1010_04-05 & 1006_11&13 to _16
WINDOW DIAGRAMS ACN 10 to 50%	- Isocratic; AmFm 10% and MeOH 0% - Isocratic; AmFm 15% and MeOH 0%	- 1013_01 to _05 - 1014_01 to _05
WINDOW DIAGRAMS MeOH 10 to 50%	- Isocratic; AmFm 10% and ACN 0% - Isocratic; AmFm 15% and ACN 0%	- 1016_01 to _05 - 1014_06 to _10
CRITICAL BANDS DIAGRAMS	- Isocratic; AmFm 10% - Isocratic; AmFm 15%	- 1017_01 & _02 - 1017_03 & _04
OPTIMAL ELUTION	- Isocratic; AmFm 10%, ACN 11% and MeOH 5% - Isocratic; AmFm 15%, ACN 5% and MeOH 19%	1017_06 1017_07

All the chromatograms are in Appendix D.

Table 7 lists the analyses made with the Primesep® SB 4.6 x 150 mm column and Primesep® SB 1.0 x 50 mm column (at the end of the Table).

Table 7: Optimization of the sugar phosphates separation with SIELC Primesep® SB columns

	ELUTION CONDITION	ANALYSIS NAMES
TESTS similar to Primesep	- Isocratic; AmFm (pH 3) 40% and ACN 20% - Gradient; AmFm (pH 3) 10 to 80% in 25 min and ACN 20%	- PRIM01 and 02 - PRIM03 and 04
TEST pH(AmFm) 3.5 to 2	Isocratic; AmFm 15%, ACN 10% and MeOH 10%	- 1103_02 and _07 to _09 - 1103_06 and _072 to _092
TESTS M(AmFm)		- TEST29-30
TESTS AmFm 10 to 50%	Isocratic; MeOH 10% and ACN 10%	- 1106_03 to _06 and 1107_03 to _06
WINDOW DIAGRAMS ACN 10 to 50%	Gradient; AmFm 15% during 15 min and 50% at 17 min	- 1113_16 to _20 - 1113_162 to _202
WINDOW DIAGRAMS ACN 5 to 25%		- 1117_01 to _05 - 1117_012 to _052
WINDOW DIAGRAMS MeOH 10 to 50%		- 1113_10 to _14 - 1113_102 to _142
WINDOW DIAGRAMS MeOH 5 to 25%		- 1117_07 to _11 - 1117_072 to _112
WINDOW DIAGRAMS THF 10 to 50%		- 1114_01 to _05 - 1114_012 to _052
WINDOW DIAGRAMS THF 5 to 25%		- 1127_01 to _05 - 1127_012 to _052
TESTS GRADIENT THF and ACN		- TEST36 to 40
TESTS GRADIENT MeOH and ACN		- TEST41 to 47
AmFm alone		- 1201_01
GRADIENT ACN		- TEST71 to 90
GRADIENT AmFm		- TEST91 to 110
TESTS with 1.0 x 50 mm column		- TEST53 to 70

A listing of all the gradients is in Appendix E, and chromatograms are in Appendix H.

For the external calibration, the Primesep® SB 4.6 x 150 mm column was used (Table 8).

Table 8: Analyses done for the external calibration of the sugar phosphates

SUGAR PHOSPHATES	ELUTION CONDITION	ANALYSIS NAMES
G6P	Gradient:	0222_02 to _05 & 0223_02 0222_022 to _052 & 0223_022
F6P		0222_06 to 09 & 0223_03 0222_062 to 092 & 0223_032
R5P		0222_10 to _13 & 0223_04 0222_102 to _132 & 0223_042
DHAP		0222_14 to _17 & 0223_05 0222_142 to _172 & 0223_052
PGA		0224_ 07 to _11 0224_ 072 to _112
FBP		0224_12 to 16 0224_122 to 162
RuBP		0224_02 to _06 0224_022 to _062

t [min]	AmFm [%]	ACN [%]	H_2O [%]
0	15	21	64
11	15	21	64
12	30	21	49
19	30	21	49
20	50	10	40
32	50	10	40
33	15	21	64

3. Results and discussion

3.1. LC-MS/MS method development

3.1.1. Optimization of the separation with SIELC Primesep® B2 columns:

The principal goal of optimizing a separation is to find an adequate resolution of the compounds of a mixture in the shortest possible time. Establishing the optimum conditions by trial and error is inefficient and relies heavily on the expertise of the analyst. Gradient elution is sometimes used as a preliminary step to indicate possible isocratic conditions. [13]

The first important step was to determine which buffer to use. For an LC/MS method, it is recommended to use a volatile buffer. Knowing that the column pH range is 1.5 to 7 [3], there are two possible buffers for those conditions:

- ammonium formate (buffer range 2.8 to 4.8) and
- ammonium acetate (buffer range 3.8 to 5.8) [6].

Recommendations of the manufacturer indicated that the column would work better at low pH [3], so ammonium formate (AmFm) seemed to be the best candidate. Thus, the only parameter needing optimization was the pH to use in the buffer. Two different pH values were tried: 3 and 2.5. The results showed that the separation worked better at pH 3 [Appendix D].

Several gradients were tried to evaluate the effect of different eluents [Appendix A]. The results were promising, especially for the separation of the three last peaks (PGA, FBP and RuBP), for which high amounts of AmFm lead to better peak shape and shorter retention times. However, none of the gradients tested resulted in a baseline separation of the four first peaks (G6P, F6P, R5P and DHAP).

To reach a better optimization of the separation, a more systematic way was then followed: the window diagrams.
The window diagram is a technique that allows optimizing one parameter after another by varying the chosen parameter and reporting the retention time variations towards this parameter. [14]

The elution composition was the first variable to be optimized. Two organic solvents were tested: acetonitrile (ACN) and methanol (MeOH). Retention time variations obtained with different buffer and solvent concentrations are reported in Figure 7, 8 and 9 [Appendices B and D for tables and chromatograms].

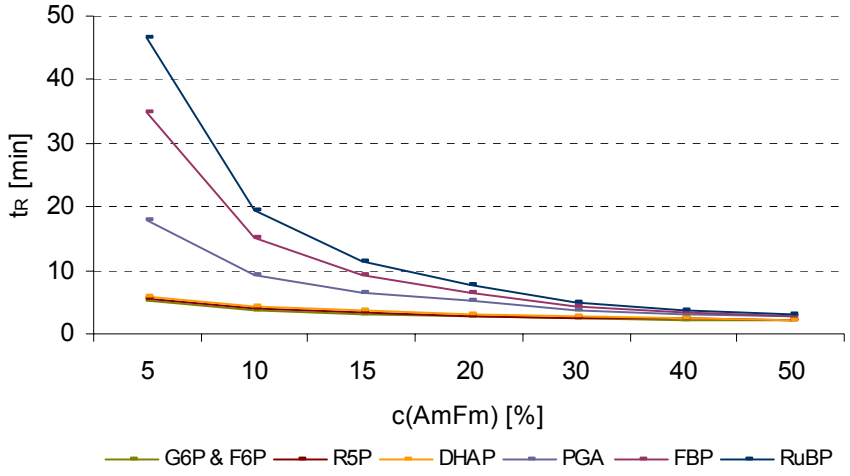

Figure 7: t_R =f(c) for different AmFm concentrations in 10% aq. ACN and 10% aq. MeOH (v/v) [Chromatogram files 1010_04-05 and 1006_11 & 13 to 16]

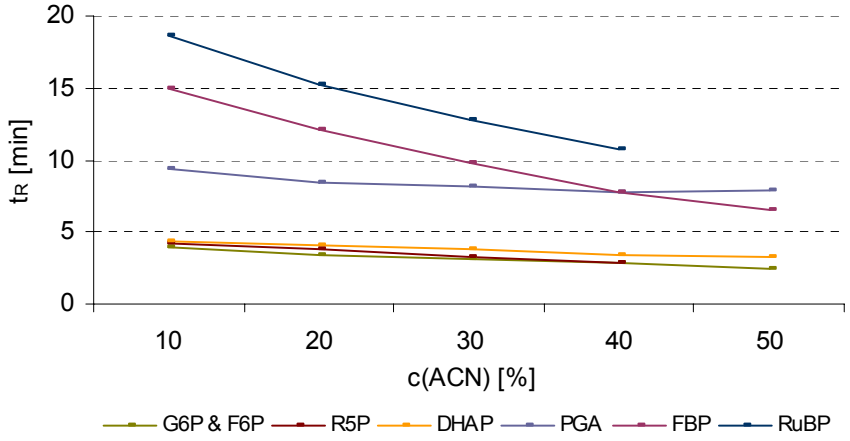

Figure 8: t_R =f(c) for different ACN concentrations in 10% aq. AmFm (v/v) [Chromatogram files 1013_012 to 05]

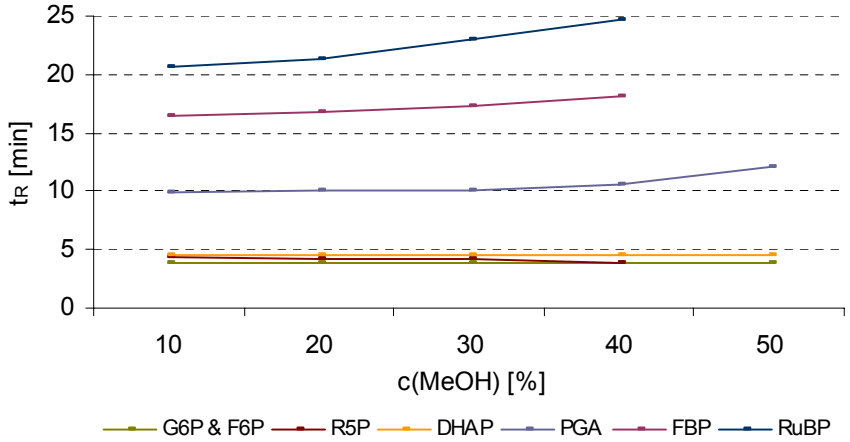

Figure 9: t_R =f(c) for different MeOH concentrations in 10% aq. AmFm (v/v) [Chromatogram files 1016_01 to 05]

Under all conditions tested, the two hexose phosphates (G6P and F6P) co-eluted. In addition, RuBP and DHAP were only partially separated.

Figure 7 demonstrates nicely that the total run time was sped up with increasing AmFm concentrations. Above 20% AmFm the analytes co-eluted. The best peak shapes were obtained at 10 and 15% AmFm and these concentrations were used for further optimization.

Figures 8 and 9 represent the results obtained with the 10% concentration. The Tables and graphs for an AmFm concentration of 15% are reported in Appendix B.

The biggest difference observed between the two AmFm concentrations is the diminution of the retention times at 15%. For example, for ACN 10%, RuBP eluted at 11 min instead of 18.6 min. In general, the retention times were roughly 1.6 times shorter at 15 than at 10%, but the resolution was better at 10%.

The graphs in Figures 8 and 9 clearly demonstrate that, compared with MeOH, ACN results in a superior separation, particularly with regard to reducing the total analysis time.
The use of high concentrations of organic solvents resulted in dramatically reduced signals for sugar phosphates. The sugar phosphates were detected at [M] masses instead of [M-H], an observation that we can not explain at present (values missing in Fig. 8 and 9).

Interestingly, with increasing ACN concentrations, we observed an inversion of the order in which PGA and FBP eluted. This characteristic could be used to shorten the analysis when only FBP is studied.

The second step of the window diagram technique consists by calculating the minimal selectivity (α), based on following equation:

$$\alpha = \frac{k'_2}{k'_1} \quad \text{with} \quad k' = \frac{t_R - t_0}{t_0},$$

t corresponding to the retention time and k' to the capacity factor.

To obtain the minimal selectivity, the calculation is made with the most difficult to separate pair of compounds (closest retention times). [14]

For the Primesep® B2 column, t_0 is 2.0 min, and because G6P and F6P could not be separated, they are considered as one peak. The calculation is made considering k'_2 as k'(R5P) and k'_1 as k'(G6P & F6P), except for ACN 40% where the calculation is made with k'(FBP) and k'(PGA).

The variation of the minimal selectivity for the different solvents is shown on Figure 10.

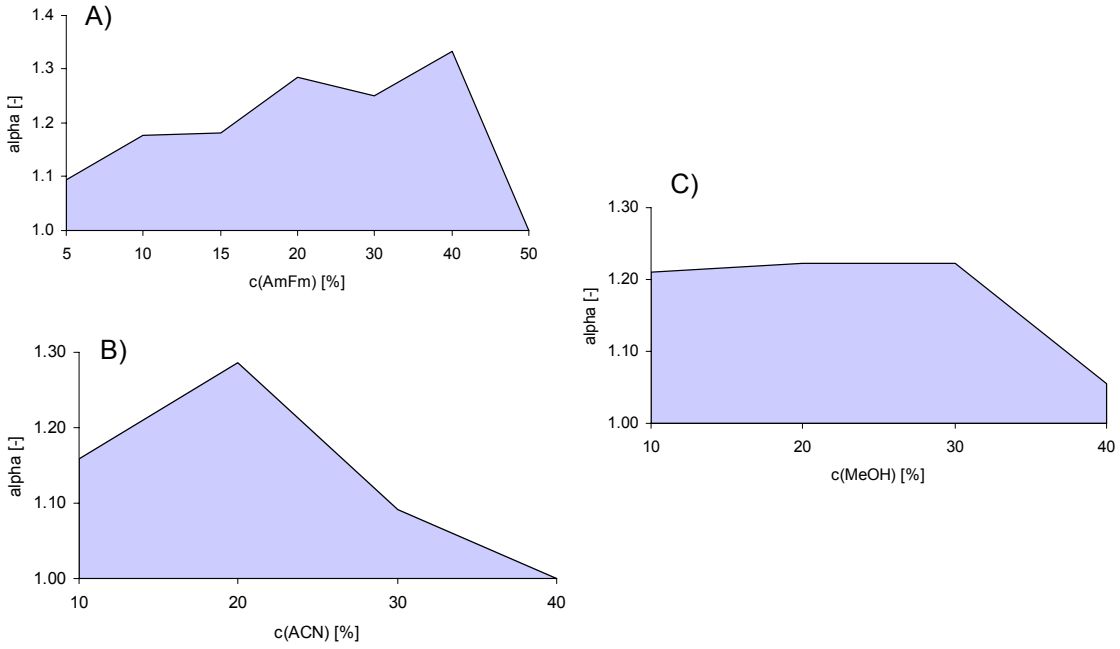

Figure 10: Window diagrams deduced from the retention time variation when different AmFm (A), ACN (B) and MeOH (C) concentrations were used

Unfortunately, the minimal selectivity approach yielded inconsistent results. For example, according to Figure 10A, the AmFm concentration with the highest minimal selectivity was 40%. However, the separation was not effective at that concentration (Fig. 7). In fact, the values of the minimal selectivities are all very close (between 1 and 1.3) for each solvent and were thus not helpful in deciding at which concentration the separation was more effective. The only general conclusion that can be made with this technique is that the separation seems to be better at low concentrations of organic solvent, because the lowest minimal selectivity values were calculated for 40 % of MeOH and ACN.

An alternative technique for optimizing the separation is based upon the use of critical bands diagrams. [15]

This technique was developed for the optimization of separations in reversed-phase liquid chromatography using binary solvents. We consider the technique applicable on our case, because the mixed-mode phase column is behaving, at least in part, like a reversed-phase column.

Although all eluents tested actually contained three components (AmFm, H_2O and an organic solvent), the concentration of AmFm was kept constant, whereas

the percentages of the two solvents were changed. This reduction to a binary solvent system enabled us to use the critical bands diagram approach.

The graphical procedure is based on the linearity of the plots of log k' against solvent composition (Colin et al. in 1983 [15]).

The first step is to plot the log k' values obtained with two binary solvent compositions, and then to draw the straight lines for each compound joining the log k' values. Then, knowing the average column efficiency and the resolution needed, a second line is drawn for each compound. This line is parallel to and below the first one. The zones delineated by the lines are called critical bands.
Then, in order to obtain the best resolution between two solutes, the solvent composition must be chosen in the region where the critical bands do not overlap. [15]

The choice of the compositions of the binary solvents is made according to the previous results, and, because the retention times are consistent, the two lines are so close to each other that they appear as one thick line.

Based upon the results shown in Figures 8 and 9, the solvent compositions chosen were 20:70 methanol-water and 15:75 ACN-water for 10% AmFm, and 25:60 methanol-water and 20:65 ACN-water for 15% AmFm. The critical bands diagrams are showed respectively on Figures 11 and 12. [Appendices B and D for tables and chromatograms]

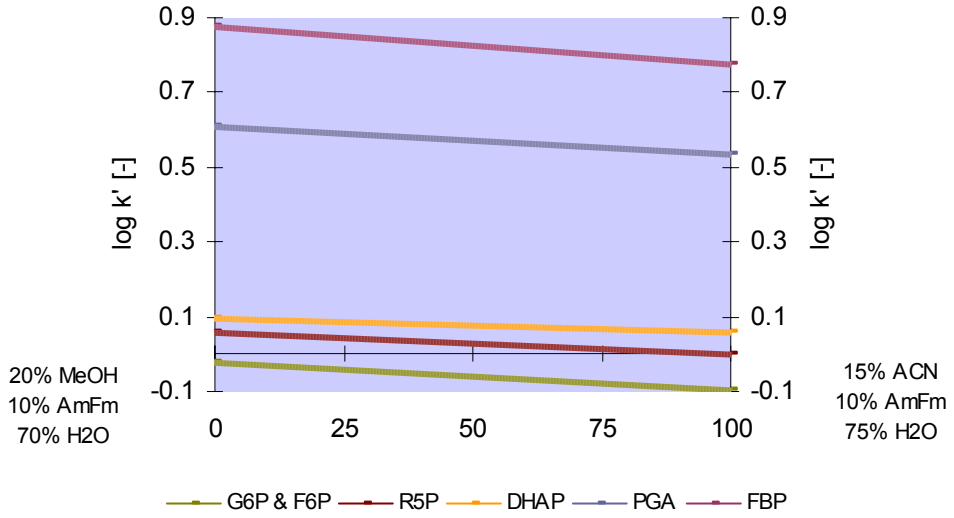

Figure 11: Critical bands diagram for the optimal concentration in 10% aq. AmFm (v/v) [Chromatogram files 1017_01-02]

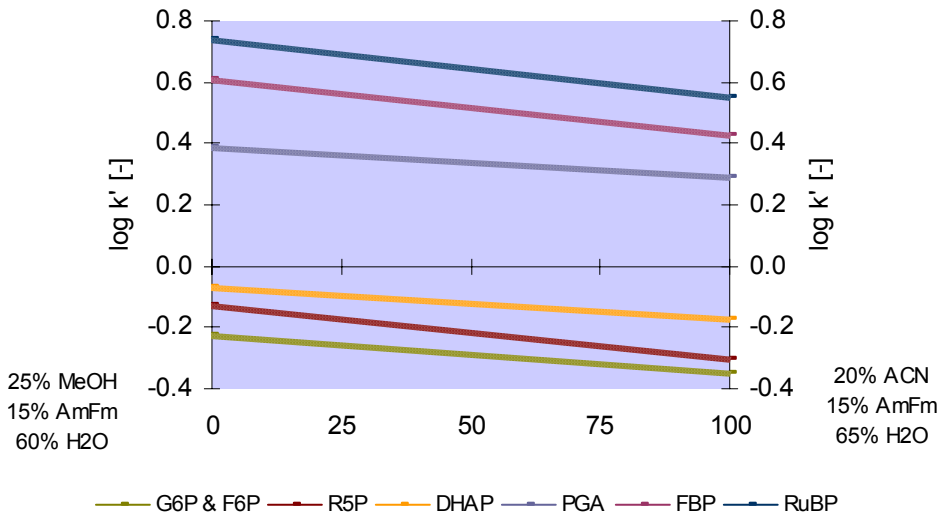

Figure 12: Critical bands diagram for the optimal concentration in 15% aq. AmFm (v/v) [Chromatogram files 1017_03-04]

According to Figures 11 and 12, the critical bands do not overlap, and are quite different regardless of the solvent composition.

Knowing that the most difficult area of the separation concerns the four first peaks and wishing that the elution remains isocratic, the optimal percentages are chosen as follow: 75% of 15:75 ACN-water for AmFm 10% and 15% of 20:65 ACN-water for AmFm 15%, which yields the concentrations of solvents listed on Table 9.

Table 9: Optimal concentrations with isocratic elution on Primesep® B2 column

AmFm [%]	ACN [%]	MeOH [%]	Analysis names
10	11	5	1017_06
15	5	19	1017_17

A complete optimization should have also included parameters such as column length, flow rate particle size and properties of the stationary phase. But, very often chromatographers are mainly interested in finding the solvent composition working with the column available. Thus, although this approach does not represent a complete optimization of the chromatographic conditions, it is a very simple way to determine the solvent composition which satisfies the needs of the analyst. [15]

The result of the optimization for 15% AmFm is shown in Figure 13 (concentration of each sugar phosphate is roughly $4 \cdot 10^{-3}$ M).

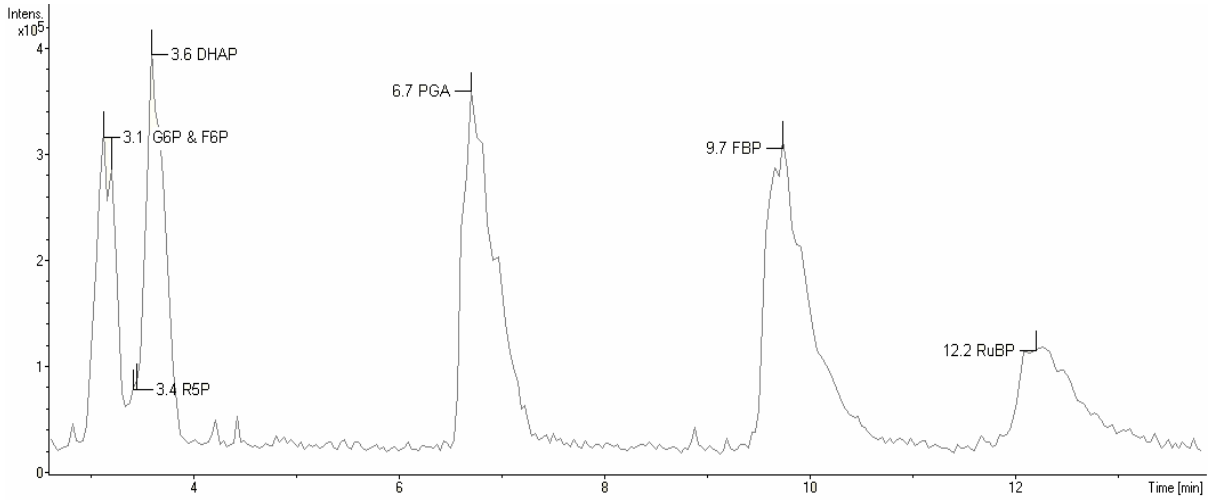

Figure 13: Total ion current chromatogram of the optimal separation with Primesep® B2 4.6 x 150 mm column [Chromatogram file 1017_17]

The chromatogram in Figure 13 shows that the three last peaks have an unsymmetrical shape. Tailing peaks are a common problem in reversed phase chromatography, and are associated with lower resolution, reduced sensitivity compromised quantification. Tailing can be caused by the fact that the sample solvent is stronger than the mobile phase or by a sample mass overload. Knowing that the samples were dissolved in the mobile phase and that the overloading is barely possible (first peaks would be influenced too), the reason for tailing is unclear. We were also working with a novel column material with limited knowledge about its properties.

The separation of the four first peaks was not as desired, which can be shown by calculating the resolution (R_s) between peaks. Furthermore, one can also calculate the column efficiency which is represented by the theoretical plate number (N).

$$R_s = 2 \cdot \frac{\left(t_{R,2} - t_{R,1}\right)}{\omega_2 + \omega_1} \text{ and } N = 16 \cdot \left(\frac{t_R}{\omega}\right)^2,$$

ω corresponding to the peak width and t_R to the retention time.

Resolution values above 0.8 are generally considered as acceptable [14]. If lower values are calculated, the separation is considered insufficient. It should be noted that the equation for the theoretical plate number does not consider the shape of the peaks (this calculation is made for symmetrical peaks). Thus, the values obtained are just approximate values.

The resolution and column efficiency details for all analytes are listed in Table 10.

Table 10: Resolutions between the peaks and theoretical plate numbers for the 1017_07 chromatogram

	G6P	F6P	R5P	DHAP	PGA	FBP	RuBP
R_s [-]	0.4	1.3	0.7	4.8	3.4	2.3	
N	2670	5060	12840	900	1120	1630	1550

The average theoretical plate number is then 3680. However, the N values being so different for each peak, this average value is just an additional indication that will be used for the comparison of the different columns.
The resolution values between G6P/F6P and R5P/DHAP are under the acceptable range (0.4 and 0.7 respectively).

Based on the disappointing results with the Primesep® B2 4.6 x 150 mm column, it was decided not to attempt to scale down the separation using the available Primesep® B2 1.0 x 50 mm column. Instead, further methods development was focused on using Primesep® SB columns.

3.1.2. Optimization of the separation with SIELC Primesep® SB columns:

During a HPLC method development, even if the stationary phase plays a dominant role in the overall retention process, the choice of the solvent also affects many parameters as the peak shape or the functional group selectivity. To choose an appropriate eluent, it is important to know the solvent chemical properties and the way they affect the chromatographic process.
For example, viscosity is a chemical property that has an effect on the backpressure monitored at the head of the column, on the flow path through the system and the flow rate. The miscibility of the solvent can also be a problem, especially when water is used. And finally, volatility has to be considered, especially when a MS detector is used. [16]

The common solvents in reversed-phase chromatography are ACN, MeOH, tetrahydrofuran (THF), water, isopropanol, ethanol, dioxane and acetone [14]. To determine the choice of the solvent mixture, two factors had to be considered: the miscibility in water and a low viscosity (because we work at low temperature, 4°C). Three solvents were chosen to be tested: ACN, MeOH and THF.

The different properties of those solvents are listed in Table 11.

Table 11: Properties of some solvents used in reversed-phase chromatography [14 and 16]

SOLVENT	VISCOSITY at 25°C [cP]	SOLUBILITY IN WATER [%]	ELUOTROPIC STRENGH S*	SOLVENT STRENGTH PARAMETER P'	GROUP OF SELECTIVITY	STABILITY
ACN	0.34	100	3.1	5.8	V	
MeOH	0.54	100	3.0	5.1	II	
THF	0.46	100	4.4	4.0	III	can form peroxides

Solvents are divided in eight different groups of selectivity according to their capacities to accept or donate protons and their tendency to form dipole-dipole interactions with the solute. The groups the most likely used in reversed-phase chromatography are theoretically II, III and VI. [14]
However, because of its nearly ideal spectroscopic qualities, coupled with excellent solubilizing capabilities and unique chromatographic properties, ACN (group V) is also a choice solvent in reversed-phase chromatography. [16]

Watching the ESI source, we noticed that the spraying process was not working optimally at 1 ml/min (drops visible in the particle spray). Thus, the nebulizer pressure and the drying gas flow were increased to 50 psi and 8 l/min. and different eluent flow rates at 0.6 and 0.8 were tested. It appeared that the optimal flow rate with Primesep® SB 4.6 x 150 mm column was 0.6 ml/min.

Before optimizing the organic solvent composition, some further analyses were performed to evaluate the effect of the pH on peak shape. Knowing that the three first peaks (G6P, F6P and R5P) were the most difficult to separate, we tried to modify the buffer pH. pH values 2, 2.5, 3 and 3.5 were tried, and, as shown in Figure 14, the best separation occurred at pH 2, where the resolution between the peaks was calculated to be 0.8 and 1.2.

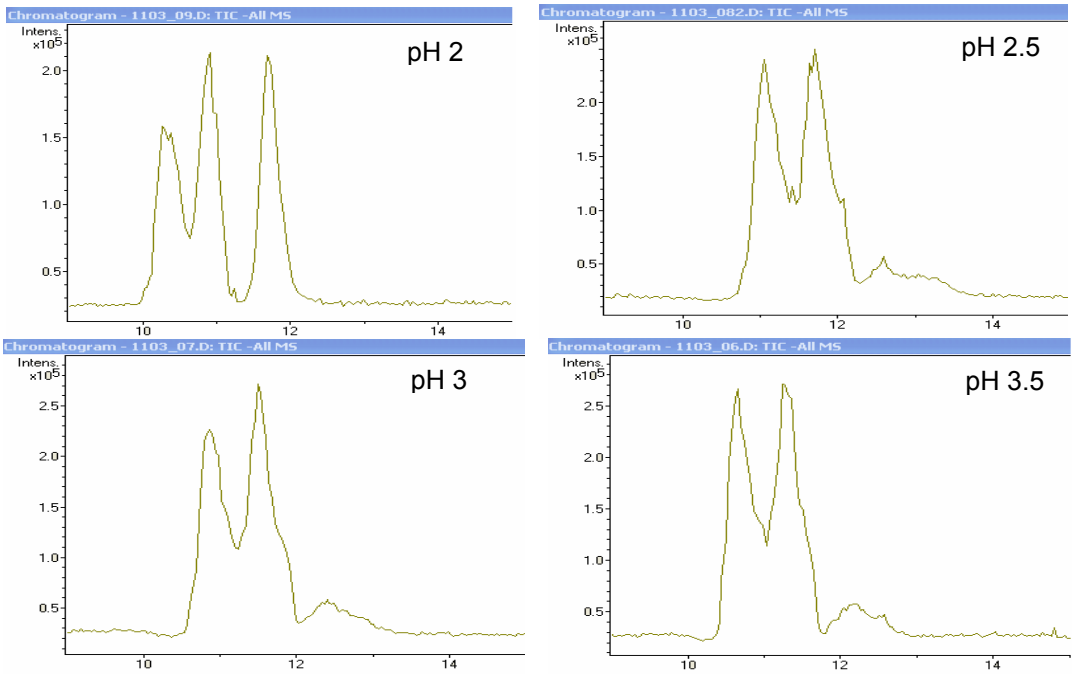

Figure 14: Total ion current chromatograms of the tests for different pH of the buffer with Primesep® SB 4.6 x 150 mm column
[Chromatogram files 1103_09, 1103_082, 1103_06 and 1103_07]

Buffer concentrations of 10 mM, 50 mM and 100 mM AmFm were tested with all standards [Appendix H]. The total run time increased with decreasing buffer concentration and the last eluting standard (RuBP) was not detectable at all in 10 mM and 50 mM AmFm.

The analysis being longer because of the use of a lower flow rate (0.6 ml/min) and considering the observations made for the B2 column, it was chosen to proceed with a gradient elution for AmFm 100 mM pH 2.

The use of gradients represents a basic means of optimizing the process of chromatographic separation. Because conventional chromatography does not always give a satisfactory resolution of some complex mixtures, gradient chromatography was developed according to the requirements of practical needs.

The degree of separation of two compounds is given by the resolution, which depends on the partition coefficient of the two compounds. The most important factors influencing this coefficient are composition of the mobile and stationary phases, the temperature and the pressure on the column. Thus, it is important to choose the most efficient eluent to achieve the separation. The use of mobile phase gradients should lead to the shortening of the analysis and hence to the optimization of the separation. [17]

To determine the ideal initial buffer/solvent composition, isocratic elutions with 10, 15, 20 and 30% AmFm (ACN 10% and MeOH 10%) were tried with only the first three standards. It showed that the separation was ever so slightly better at 10%, but that percentage also made the analysis longer, so 15% was chosen as a compromise between quality and time. [Appendix H]

To test the optimal final buffer solvent composition, isocratic elutions of 20, 30, 40, and 50% AmFm were tried with all standards. A percentage of 50% was chosen to shorten the rest of the method development, what gives us a step gradient going from 15% AmFm during the first 15 minutes and then increased to 50% at 17 minutes till the end of the separation. [Appendix H]

To optimize the chromatographic conditions, the window diagrams method was used as mentioned before (Chapter 3.1.1). All tests were run twice to assess the reproducibility. Retention time variations observed with different solvent concentrations are reported in Figures 15 (for ACN), 16 (for MeOH) and 17 (for THF). [Appendix F for tables and graphics].

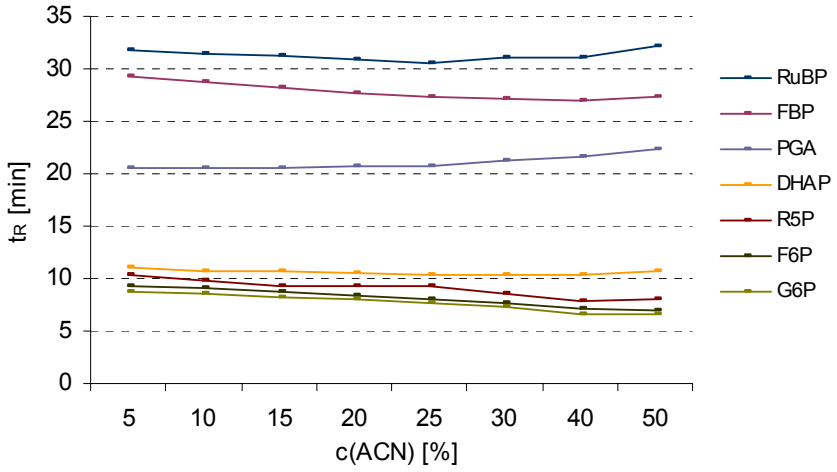

Figure 15: t_R =f(c) for different ACN concentrations in aq. AmFm [Chromatogram files 1117_01 to 05 and 1113_18 to 20]

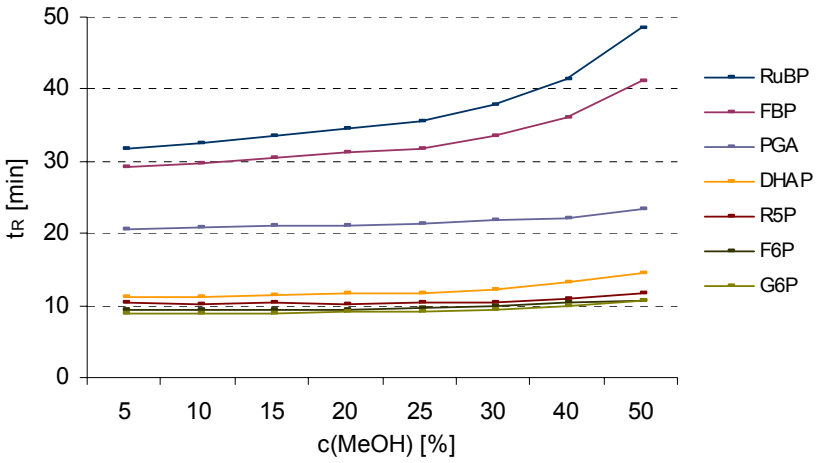

Figure 16: t_R =f(c) for different MeOH concentrations in aq. AmFm [Chromatogram files 1117_072 to 112 and 1113_122 to 142]

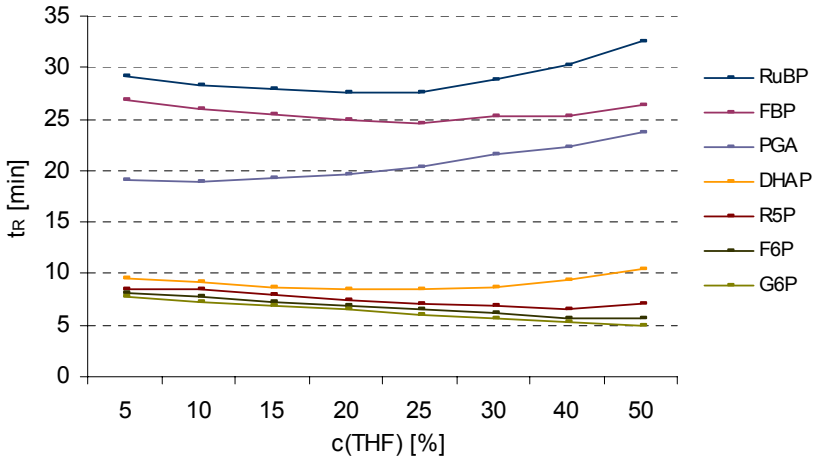

Figure 17: t_R =f(c) for different THF concentrations in aq. AmFm [Chromatogram files 1127_012 to 052 and 1114_032 to 052]

The two hexose phosphates were separated at almost all different concentrations.

We can also observe that the amount of ACN or THF doesn't really influence the separation. Indeed, except at high organic solvent concentration, the retention times are quite constant for each elution. The influence of MeOH on the contrary is more visible, but it increases the analysis time. Anyway, these results confirm those obtained with the B2 column, establishing that AmFm is the parameter with the most pronounced influence on the separation.
At high organic concentrations, some of the sugar phosphates were sometimes not detectable at [M-H] but at [M]. Thus, even if for high percentages of organic mobile phase the separation appeared to be quite good, the sensitivity of detection was compromised.

From the results shown in Figures 15, 16 and 17, the minimal selectivity was calculated. In all chromatograms, the critical pair was G6P/F6P. The dead volume measured for the Primesep® SB 4.6 x 150 mm column was 3.2 min.

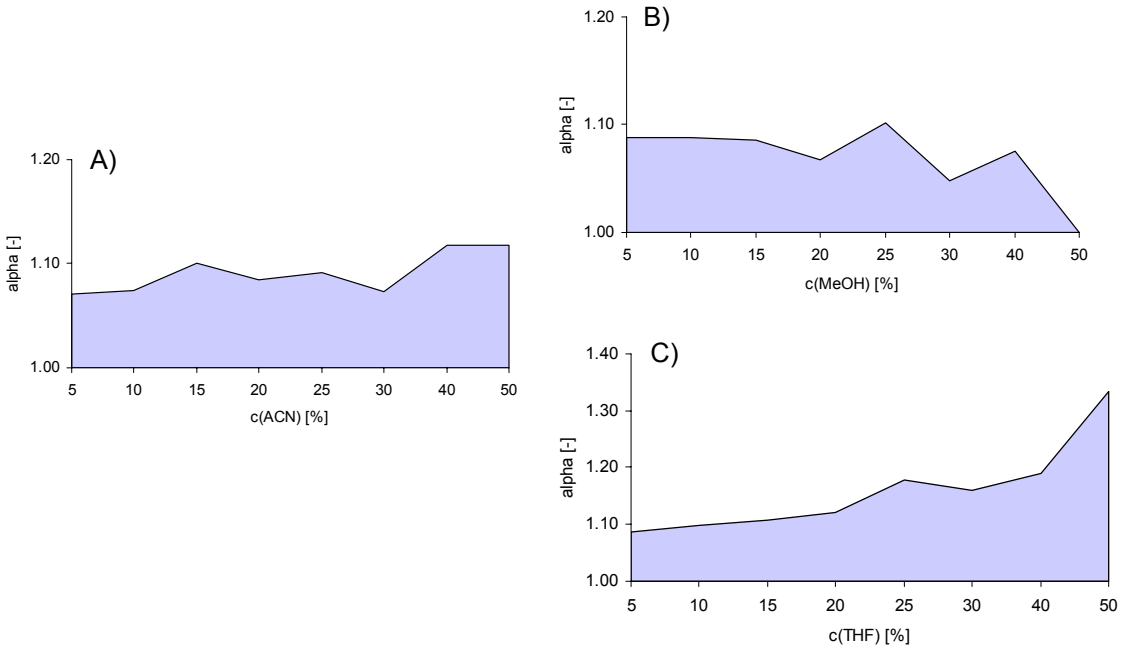

Figure 18: Window diagrams deduced from the retention time variation when different ACN (A), MeOH (B) and THF (C) concentrations are used

As for the Primesep® B2 4.6 x 150 mm column, the selectivity is not a helpful parameter to choose the optimal organic concentrations, except with THF, but the highest minimal selectivity (1.33) is at a concentration (50% THF) where some standards (G6P, F6P, R5P and RuBP) are not detected at the right mass-to-charge ratio. Thus, for generating the critical bands diagrams, we arbitrarily chose 10% THF, 20% ACN and 5% MeOH [Appendix G].
However, since this systematic technique was not useful in this case, the effect of different solvent compositions was tested empirically.

The most challenging part of the separation was the separation of hexose phosphates and the detection of R5P. Thus, some quaternary elution compositions involving AmFm 100mM pH 2, water and two of the three organic solvents were tried with a particular attention on the first four peaks (G6P, F6P, R5P and DHAP). [Appendices E and H]
The separation was always better at low (even non-existent) concentrations of THF and MeOH and, on the contrary, the presence of ACN was necessary for the separation of the four first peaks. We could also find out that the detection of RuBP was better when a decrease of ACN concentration was applied in the middle of the analysis.

Further analyses were performed to define the optimal initial and final concentrations of ACN and AmFm with Primesep® SB 4.6 x 150 mm column.

For the initial eluent composition 15, 18, 19, 20 ,21, 22 and 25% ACN and 13, 15, 16, 17, 18, 19, 20, 21, 22 and 25% AmFm 100mM pH 2 were tried, and for the final eluent composition 5, 10 and 15 % ACN and 30, 40, 50, 60 and 70% AmFm 100mM pH 2 [Appendix E]. We also tried to find out the best time for a step change in the AmFm and ACN concentrations.

The optimal mobile phase step gradient is presented in Table 12.

Table 12: Optimal elution with Primesep® SB 4.6 x 150 mm column [TEST108]

t [min]	AmFm 100 mM pH 2 [%]	ACN [%]	H_2O[%]
0	15	21	64
11	15	21	64
12	30	21	49
18	30	21	49
19	50	10	40
32	50	10	40
33	15	21	64

It should be mentioned that the analysis can be shortened by increasing the concentration of AmFm earlier. However, sensitivity is lost, especially for the detection of PGA. Indeed, the area of PGA signal decreased almost two-fold when the concentration of AmFm was increased earlier. Thus, 40 min run time was considered as a good compromise between rapidity and sensitivity.

The chromatogram resulting from the optimal gradient is shown in Figure 19.

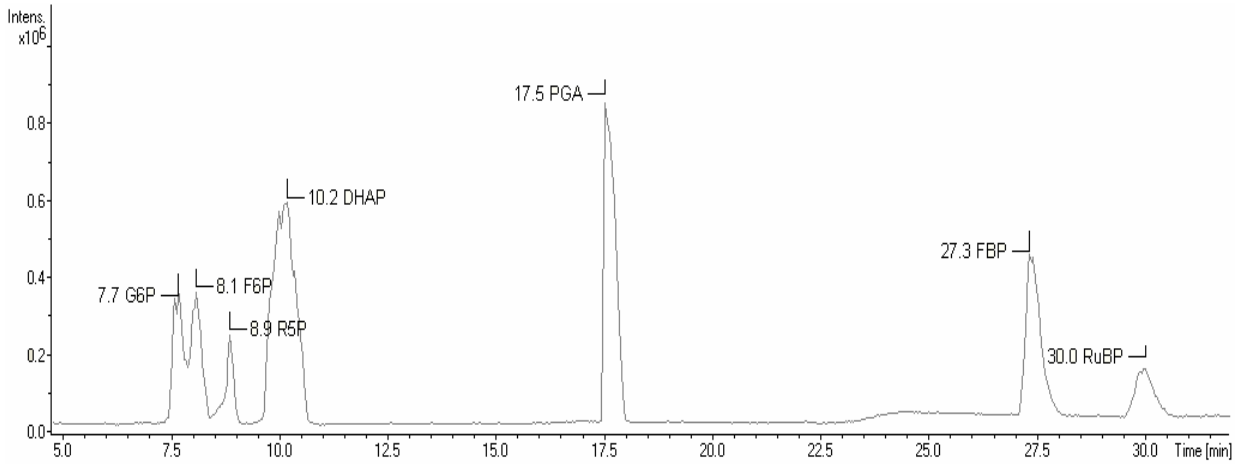

Figure 19: Total ion current chromatogram of the optimal separation with Primesep® SB 4.6 x 150 mm column [Chromatogram file TEST108]

The resolution between the peaks and the theoretical plate number were calculated and are shown in Table 13.

Table 13: Resolutions between the peaks and theoretical plate numbers for the TEST108 chromatogram

	G6P	F6P	R5P	DHAP	PGA	FBP	RuBP
R_s [-]		0.8	1.8	1.7	8.3	12.6	2.5
N	3790	4200	7920	1380	11600	14720	8520

The average theoretical plate number was 7450, and the resolution values were all equal to or higher than 0.8. Compared to the Primesep® B2 4.6 x 150 mm column, the average theoretical plate number was higher, and the resolution between the hexose phosphate peaks was in the acceptable range. R5P was previously co-eluting with the hexose phosphates or DHAP was now baseline-separated. We also observed an improved symmetry of the peaks.

The Primesep® SB 1.0 x 50 mm SB column was also tested. Different elution compositions were tried [Appendix I and J] and the best result obtained (standards at 0.05%, LC flow of 0.1 ml/min and isocratic elution of AmFm 15% and ACN 20%) is showed in Figure 20.

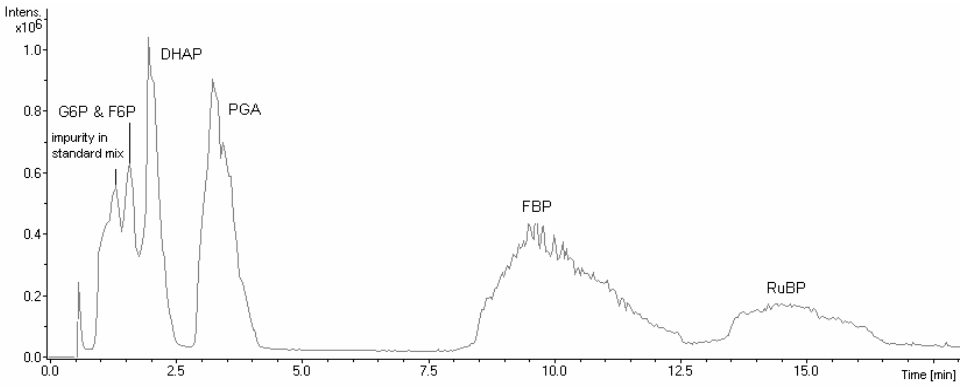

Figure 20: Total ion current chromatogram of the optimal separation with Primesep® SB 1.0 x 50 mm column [Chromatogram file TEST58]

Ideally, the use of a smaller column with the same stationary phase should give a similar separation as with the longer column but in a shorter time. Unfortunately, although shorter retention times, the separation of hexose phosphates, R5P and DHAP was not satisfactory. The peaks corresponding to sugar bisphosphates were broadened to >4 min.
This column could be used for the analysis of particular sugar phosphates when only specific mass traces are wanted. However, further optimization would have to be done concerning the eluent composition because the present results are not acceptable for most of the sugar phosphates tested.

In conclusion, out of the 4 columns tested, the Primesep® SB 4.6 x 150 mm column is definitely the best for the present separation and was thus used for all further analyses.

3.1.3. Optimization of the detector response:

During ion transport in the MS system, the ions pass first through the glass capillary where voltages at the entrance and at the end create an electrostatic gradient that supports the production of charged droplets that migrate towards the capillary exit. The skimmer removes the bulk of the drying gas and the ions then pass into an octopole ion guide that transports them to the focusing lenses, from where they pass into the ion trap. The voltages set for the skimmer, octopole (dc and rf) and exit lenses determine the ion transport efficiency as well as the background level of spurious noise events. [18]

With the Agilent ion trap detector some parameters can be optimized automatically, but in order to do the optimization, the ions are directly injected into the detector (direct infusion of analytes into solvent stream). For each metabolite the eluent composition has to match the conditions when this metabolite elutes from the column into the ion source.

It should be noted that for both DHAP and PGA ((M = 170 and 186) dimers were formed in the MS ion source ($(2M-H)^{\ominus}$ = 339 and 371) and the $(M-H)^{\ominus}$ monomers at m/z 169 and 185 were barely detectable. We tried different fragmentation amplitudes to fragment the m/z 339 and 371 ions, but the major detectable daughter ion was m/z 97 (phosphate moiety). Although the two dimer ions were detected with higher sensitivity than the regular molecular ions, the MS optimization for DHAP and PGA was performed with m/z 169 and 185, respectively.

For the other sugar phosphates, we also tried to find daughter ions to do the MS optimization. However, in full scan mode, the main daughter ion for all those sugar phosphates was always the m/z 97 (phosphate moiety) that is common to all analytes tested and consequently is not of diagnostic value for a particular sugar phosphate. The MS optimization was thus focused on the mother ions.

Each optimization experiment was run twice and the complete results are reported in Appendix K. Table 14 shows the average values for each ion.

Table 14: MS parameters optimized by the detector for each ion

	259 m/z (G6P)	**259 m/z (F6P)**	**229 m/z (R5P)**	**169 m/z (DHAP)**	**185 m/z (PGA)**	**339 m/z (FBP)**	**309 m/z (RuBP)**
Capillary [V]	4983	5000	5000	4943	5000	5000	5000
Skimmer [V]	-29.51	-22.13	-16.80	-22.13	-25.74	-18.69	-22.95
Cap.exit [V]	-61.97	-82.14	-86.97	-40.66	-75.63	-61.48	-66.40
Oct DC 1 [V]	-4.68	-2.41	-2.15	-3.94	-3.27	-2.07	-1.65
Oct DC 2 [V]	-0.70	-0.54	-0.43	-0.31	-0.33	-0.86	-0.78
Trap drive*	41.30	31.08	29.11	28.22	28.65	37.19	36.42
Oct RF [V]	69.02	43.12	44.43	52.79	51.36	45.9	46.72
Lens 1 [V]	3.33	2.12	2.22	2.36	2.86	1.32	2.13
Lens 2 [V]	55.50	40.82	39.67	39.51	42.95	35.16	43.11

* no unit given by manufacturer

It was decided to divide the chromatographic run into three segments, with optimized MS conditions set for the particular metabolites eluting during a given time segment. During the first segment, G6P, F6P, R5P and DHAP eluted, in the second segment PGA was detected and the sugar bisphosphates were detected in the last segment (Table 15).

There are two other parameters that can be optimized by the operator: the ICC (Ion Charge Control) target and the fragmentation amplitude. The ICC for example, prevents the overloading of the trap by limiting the number of ions in the trap [18]. Those parameters were optimized visually during the direct injection process.

Table 15: Optimized MS method

MS Parameters	**Segment 1 5 to 12.5 min**	**Segment 2 14 to 21 min**	**Segment 3 26 to 33 min**
Capillary [V]	5000	5000	4700
Skimmer [V]	-19	-20	-20
Cap. exit [V]	-80	-75	-80
Oct DC 1 [V]	-2	-2	-1.9
Oct DC 2 [V]	-0.5	-0.33	-0.82
Trap drive*	30	28	37
Oct RF [V]	45	43	46
Lens 1 [V]	2.2	2.2	1.5
Lens 2 [V]	40	36	36
ICC Target*	20000	20000	20000
Frag. Ampl. [%]	20	40	40

* no unit given by manufacturer

Between these time segments (from 0 to 4.9 min, 12.6 to 13.9 min, 21.1 to 25.9 min and 33.1 to 40 min) the HPLC flow goes to waste and the nebulizer is set to 15 psi.

Our initial efforts focused on using the Auto MS/MS mode, in which all ions detected above a certain threshold intensity are fragmented. In contrast, in multiple reaction monitoring mode (MRM) only prespecified target ions are further fragmented, thus allowing for highly sensitive quantifications.

The MRM experiment is accomplished by specifying the parent mass of the compound(s) for MS/MS fragmentation and then specifically monitoring for a single fragment ion. When only one parent mass is chosen, it is called selected reaction monitoring (SRM). [19]

Some examples of the spectra obtained with MRM mode for each standard are visible in Figure 21. [Appendix L]

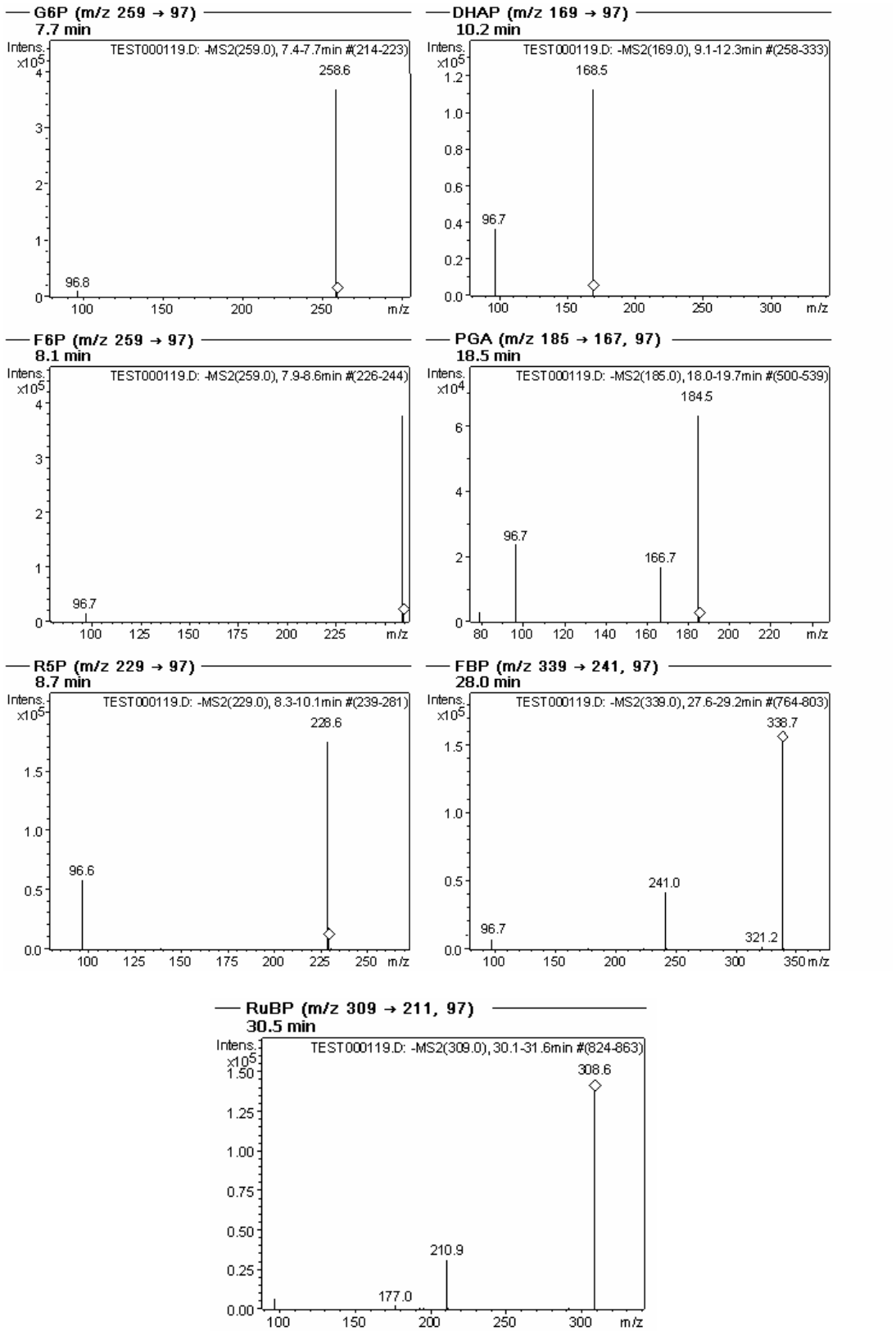

Figure 21: MRM spectra for G6P, F6P, R5P, DHAP, PGA, FBP and RuBP [Chromatogram file TEST119]

A standard mix (~0.02% for F6P, G6P, R5P, DHAP and PGA, and ~0.01% for FBP and RuBP, dilution 10 times from the stock solution) was run using the optimized method (Fig. 22). [Appendix L]

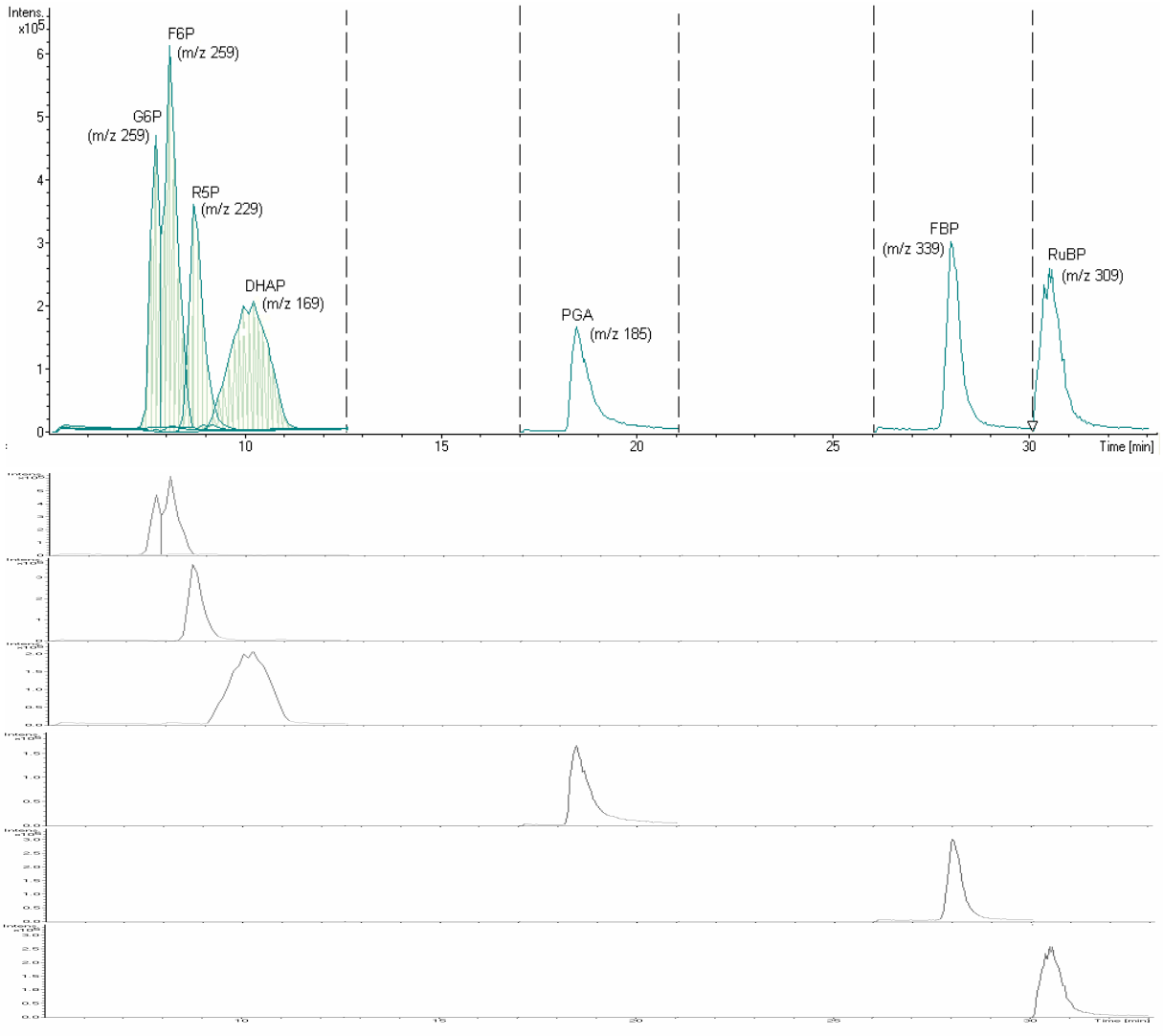

Figure 22: MRM chromatogram of the complete optimal separation and single ion traces for m/z 259, 229, 169, 185, 339 and 309 [Chromatogram file TEST119]

The height of the peaks corresponding to DHAP and PGA were smaller than in previous chromatograms. This is due to the fact that peaks were detected at $(M\text{-}H)^{\ominus}$, whereas previous runs showed the signals for dimers $(2M\text{-}H)^{\ominus}$.

The separation of the four first peaks is slightly compromised, but, because of the use of MRM mode, the specific ion traces gave excellent results, except for the hexose phosphates which have the same mass (Fig. 22).

3.2. Calibration of the detector response

As for the optimization of the detector response, the calibration was executed with Primesep® SB 4.6 x 150 mm column. An external calibration was performed for each standard and gave the calibrations curves on Figure 23.

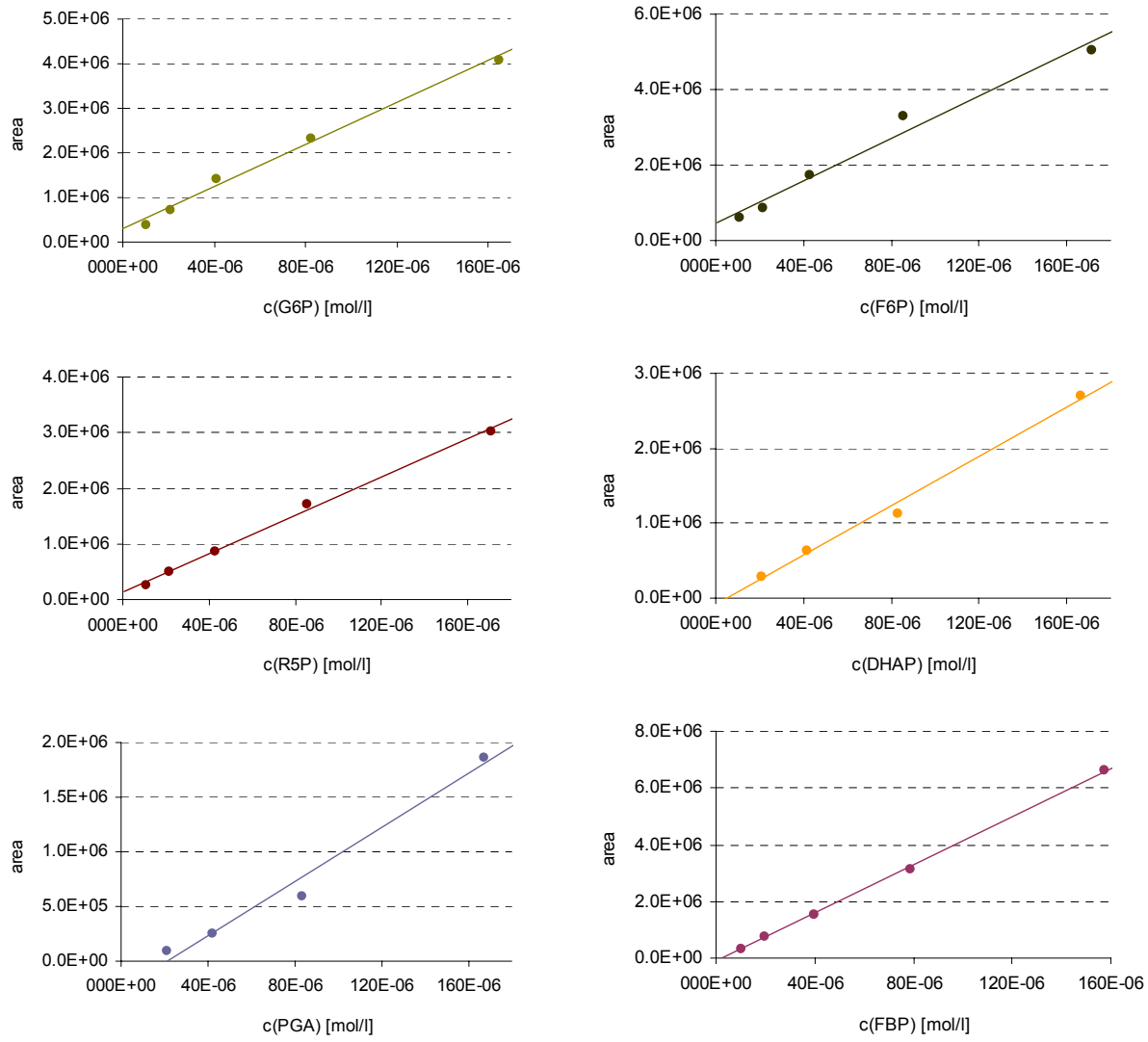

Figure 23A: Calibration curves for G6P, F6P, R5P, DHAP, PGA and FBP [Chromatogram files 0222_02 to 17, 0223_02 to 04, 0224_082 to 112 and12 to 16]

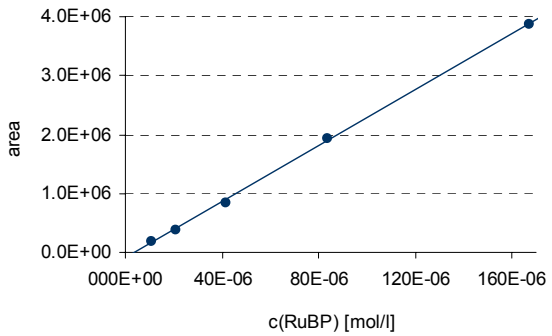

Figure 23B: Calibration curve for RuBP
[Chromatogram files 0224_03 to 06]

A statistical analysis was performed on each calibration graph. The equation for the linear regression is $y = c_0 + c_1 \cdot x$. The standard deviation (s_{yx}) and the deviation of the regression coefficient (s_{c1} and s_{c0}) were calculated following the equations ($\hat{y}$ corresponding to the y calculated with the equation of the regression and N corresponding to the number of points):

$$s_{yx} = \left| \sqrt{\frac{\sum_{i=1}^{N} (\hat{y}_i - y_i)^2}{N-2}} \right| ; \; s_{c_1} = \pm \frac{s_{yx}}{\sqrt{\sum_{i=1}^{N} x_i^{\,2} - N \cdot \bar{x}^2}} \text{ and } s_{c_0} = \pm \sqrt{\frac{\sum_{i=1}^{N} x_i^{\,2}}{N}} \cdot s_{c_1}$$

The coefficient of correlation (R) can be calculated too, following the equation:

$$R = \left| \frac{\sum_{i=1}^{N} (x_i - \bar{x}) \cdot (y_i - \bar{y})}{\sqrt{\sum_{i=1}^{N} (x_i - \bar{x})^2 \cdot \sum_{i=1}^{N} (y_i - \bar{y})^2}} \right|$$

The correlation between the variables was checked using the Student's *t*-test.

$$t = \frac{R \cdot \sqrt{N-2}}{\sqrt{1-R^2}} .$$

This *t* value is then compared with the theoretical *t* value for a level of significance of 0.05. If $t > t_{0.05,\,N-2}$, the variables x (concentration) and y (area) are correlated. [20]

The results of all calculations are listed in Table 16. [Appendices M for tables and graphs].

Table 16: Regression results and statistical calculations

SUGAR PHOSPHATES	EQUATION	R [-]	t	$t_{0.05, N-2}$
G6P	area = (3 ± 1) · 10^5 + (24 ± 1) · 10^9 · c [mol/l] (1.5 · 10^5; 95%; 5)	0.996	19.906	3.182
F6P	area = (5 ± 2) · 10^5 + (28 ± 3) · 10^9 · c [mol/l] (3.2 · 10^5; 95%; 5)	0.99	11.401	3.182
R5P	area = (13 ± 5) · 10^4 + (172 ± 6) · 10^8 · c [mol/l] (8.0 · 10^4; 95%; 5)	0.998	27.903	3.182
DHAP	area = (-1 ± 1) · 10^5 + (16 ± 1) · 10^9 · c [mol/l] (1.2 · 10^5; 95%; 4)	0.996	15.601	4.303
PGA	area = (-3 ± 1) · 10^5 + (12 ± 1) · 10^9 · c [mol/l] (1.5 · 10^5; 95%; 4)	0.99	9.330	4.303
FBP	area = (-10 ± 5) · 10^4 + (424 ± 6) · 10^8 · c [mol/l] (7.3 · 10^4; 95%; 5)	0.9997	69.510	3.182
RuBP	area = (-8 ± 3) · 10^4 + (238 ± 4) · 10^8 · c [mol/l] (4.7 · 10^4; 95%; 5)	0.9996	64.651	3.182

The linear correlations were obtained for all sugar phosphates (Table 16). The calibration curves for DHAP and PGA were calculated only with four points because the detection was severely compromised at low concentrations. However, the detection of these sugar phosphates is not a problem, because their dimers can be detected with ease.

The detection limit is the amount or concentration of an analyte that gives a signal that is 2-3 times the noise [4]. At a ratio of 3:1, the detection limits were 74 pmoles for G6P, 64 pmoles for F6P, 89 pmoles for R5P, 155 pmoles for DHAP, 140 pmoles for PGA, 32 pmoles for FBP and 83 pmoles for RuBP. [Appendix M]

Those detection limits and the calibration process can be considerably improved by the use of an internal standard. Internal standards should have very similar chemical properties compared to the analytes. For example, an isotopically labeled standard of the molecule will have a similar extraction recovery and a similar ionization response. However, such compounds can be very expensive and a chemical synthesis might be difficult. [19]

Another possibility would be to find a sugar phosphate not involved in the photosynthesis pathway but with similar properties to the sugar phosphates analysed.
Previous works on sugar phosphates quantification used 5-thio-D-glucose-6-phosphate or $^{13}C_6$-D-glucose-6-phosphate as internal standards. [12-21]

Concerning the repeatability and reproducibility, the retention times and areas were always very consistent. [Appendices B, D, F, H and M]

3.3. Applications

The method was tested on a biological sample. Sugar phosphates were extracted from tobacco leaf following the extraction process reported in Appendix O. The chromatogram is shown in Figure 24.

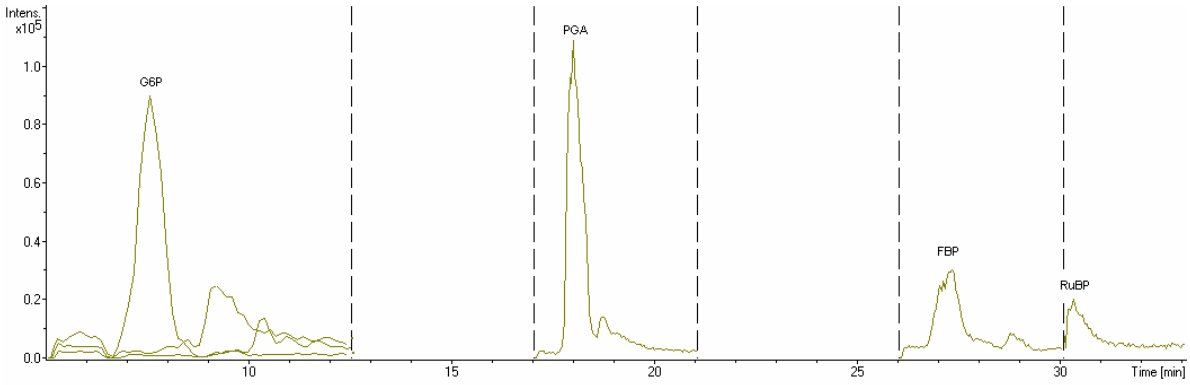

Figure 24: MRM chromatogram of a biological sample
[Chromatogram file WTMAR020003]

Four sugar phosphates were detected in the extract: G6P, PGA, FPB and RuBP.

Interestingly, the retention times were found to be shifted compared to the elution with a standard mix. For example, for FBP, the retention time with the standard separation was 28.0 min (Fig. 22), but, when the plant extract was injected, a retention time of 27.3 min was obtained. To assess if the reason of this shift was due to the matrix effect, a small quantity of standard was spiked into the biological sample.

It should be noted that in full scan mode, a large quantity of impurities was detected and some of those impurities were still detected in MRM mode, which might explain the unsatisfactory peak shapes.

With all those observations, it was decided not to attempt quantification as long as those factors would not be improved.

Anyway, this method will be potentially faster, more sensitive and less expensive than the current techniques for quantification of sugar phosphates from plants samples such as enzymatic techniques [22] or thin layer chromatography (radioactive labeling required).

4. Conclusions

The HPLC-ESI- MS/MS method using mixed-mode stationary phase proved to be a successful approach towards separation of sugar phosphates. The Primesep® SB 4.6 x 150 mm column was found out to be the most efficient column. The pH of the mobile phase and the use of a buffer were critical parameters for obtaining good separation and peak shape. The separation was confirmed by the calculation of the resolutions and the detector response was optimized to allow detection of low concentrations. The method was successfully validated by determining the linearity and sensitivity, and observing repeatability and reproducibility. Finally, the detection in a biological sample will lead to a quantification of the sugar phosphates involved in the Calvin-Benson cycle and allow a better comprehension of this pathway.

5. Acknowledgments

Mark Lange, for having been a helpful and flexible supervisor;
Jeff Cruz, for his work on the biological part of the project;
Matthias Wüst, for having offered me the opportunity to come in Pullman;
Teresa Docimo, for a constant support;
All the members of Mark Lange's Lab, for the nice working environment, and
All my friends in Pullman, for making that experience unforgettable.
Thanks!!

6. References

1. Mermet, Otto, Valçarel, Kellner and Widmer, *Analytical Chemistry*, Wiley-VCH, Weinheim (2004), p. 558 to 567, 823 to 864 and 884 to 890.
2. Skoog, West and Holler, *Chimie analytique*, DeBoeck Université, Paris (1997), p. 701 to 707.
3. SIELC homepage, http://www.sielc.com/
4. Niessen and van der Greef, *Liquid Chromatography – Mass Spectrometry*, Marcle Dekker, New York (1992).
5. De Hoffmann, Charette and Stroobant, *Spectrométrie de masse*, Dunod, Paris (1999).
6. Marvin C. McMaster, *LC/MS: A Practical User's Guide*, John Wiley & Sons, Inc, New York (2005).
7. Niessen, W. M. A., *Liquid Chromatography – Mass Spectrometry*, Marcle Dekker, New York (1999).

8. Wikipedia, The free Encyclopedia, http://en.wikipedia.org/wiki/Photosynthese
9. Buchanan, B. B., Gruissem, W., and Jones, R. L., *Biochemistry and Molecular biology of plants*, American Society of Plant Physiologists, Rockville, MD (2000), p. 610 to 620.
10. Department of Bacteriology, University of Wisconsin-Madison, USA, Microbiology Web textbooks, *Carbon Assimilation*, http://www.bact.wisc.edu/Microtextbook/index.php?name=Sections&req=viewarticle&artid=63
11. Department of Biology, University of Hambourg, Germany, Botany online, *The Dark Reactions of Photosynthesis, Assimilation of Carbon Dioxide And The Calvin Cycle* (2003), http://www.biologie.uni-hamburg.de/b-online/
12. Vas, G., Conkrite, K. et al., *Study of transaldolase deficiency in urine samples by capillary LC-MS/MS*, J. Mass Spectrom. (2006), 41: 463-469.
13. Fifield, F.W., and Kealey, D., *Principles and Practice of Analytical Chemistry*, Blackwell Science, Oxford (2000), p. 139 to 144.
14. Unpublished class material: *Chromatographie en phase liquide*, Cicciarelli, R., HEVs, Sion (2005).
15. Colin, H., Krstulovic, A., and Guidochon, G., *The Importance of Dead Volume in the Optimization of Separations in Reversed-Phase Liquid Chromatography Using Ternary Solvents*, Chromatographia (1983), 17: 209-214.
16. Sadek, P. C., *The HPLC solvent guide*, John Wiley & Sons, Inc., New York (1996).
17. Liteanu, C., Gocan, S., *Gradient Liquid Chromatography*, Ellis Horwood, Chichester (1974), p. 125 to 250.
18. Agilent 1100 Series LC/MSD Trap System, Concept Guide (2004).
19. IonSource homepage, *Principles of MS quantitation*, http://www.ionsource.com/tutorial/msquan/requantoc.htm
20. Unpublished class material: *Cours de Statistiques appliquées*, Grogg, A., HEVs, Sion (2004).
21. M.M.C., Wamelink, E.A., Struys, et al., *Quantification of sugar phosphate intermediates of the pentose phosphate pathway by LC-MS/MS: application to two new inherited defects of metabolism*, J. Chromatogr. B (2005), 823: 18-25.
22. Madhusudana, R., Norman, T., *Leaf Phosphate Status, Photosynthesis, and Carbon Partitioning in Sugar Beet*, Plant Physiol. (1989) 90: 814-819.

7. Appendices

[A] Gradients tried with Primesep® B2 4.6 x 150 mm column
[B] Window diagrams with Primesep® B2 4.6 x 150 mm column
[C] Critical bands diagrams with Primesep® B2 4.6 x 150 mm column
[D] Chromatograms of the analyses made with Primesep® B2 4.6 x 150 mm column
[E] Gradients tried with Primesep® SB 4.6 x 150 mm column
[F] Window diagrams with Primesep® SB 4.6 x 150 mm column
[G] Critical bands diagrams with Primesep® SB 4.6 x 150 mm column
[H] Chromatograms of the analyses made with with Primesep® SB 4.6 x 150 mm column
[I] Elutions tried with Primesep® SB 1.0 x 50 mm column
[J] Chromatogram and Spectra of TEST58 with Primesep® SB 1.0 x 50 mm column
[K] MS optimization results
[L] Chromatogram and Spectra of TEST119 with Primesep® SB 4.6 x 150 mm column
[M] Calibration curves and statistic calculations
[N] Chromatogram and Spectra of a tobacco leaf sample
[O] Extraction process of sugar phosphates from plants